



Conceptual design and optimization of a sustainable and environmentally friendly archetypal helicopter within the selection criteria and limitations

Enes Gunaltili^a, Selcuk Ekici^b, Abdullah Kalkan^c, Faruk Esat Gocmen^c,
Utku Kale^{d,e,*}, Zeki Yilmazoglu^f, T. Hikmet Karakoc^{g,h}

^a Department of Astronautical Engineering, Konya Necmettin Erbakan University, Konya, Turkey

^b Department of Aviation, Iğdır University, Iğdır, Turkey

^c TAI, TUSAŞ (Turkish Aerospace Industries), Ankara, Turkey

^d Department of Aeronautics and Naval Architecture, Faculty of Transportation Engineering and Vehicle Engineering, Budapest University of Technology and Economics, Budapest, Hungary

^e Faculty of Technology, Aviation Academy, Amsterdam University of Applied Sciences, Amsterdam, Netherlands

^f Department of Mechanical Engineering, Gazi University, Ankara, Turkey

^g Faculty of Aeronautics and Astronautics, Eskisehir Technical University, Eskisehir, Turkey

^h Information Technology Research and Application Center, Istanbul Ticaret University, Istanbul, Turkey

ARTICLE INFO

Keywords:

Helicopter
Conceptual and sustainable design
Sustainability
Environmentally friendly

ABSTRACT

The design and mission requirements of aero vehicles, which vary on a day-to-day basis, have become major study concerns in the burgeoning aviation sector. In addition to the design and mission criteria that must be met in an aero vehicle design, the designers' primary goals are to construct original, innovative, environmentally friendly, fuel-efficient, and sustainable designs. In this study, a detailed conceptual design of a helicopter that does not need a notable runway for operation and is limited by mission and design requirements is offered. Within the scope of this research, a competitor analysis study was undertaken in accordance with the defined criteria, and design approaches were chosen based on the outcomes of competitor analysis. In addition, this research, which looks for an environmentally friendly and sustainable design, was developed with the aviation industry's demands in mind by analyzing the International Helicopter Safety Team's (IHST) data. As a result of the reports analyzed and considering the causes and consequences of accidents that have happened, the objective of the design research was to achieve a sustainable, ecologically friendly, and fuel-efficient design by reducing the number of accidents and damage. The planning and design processes as a result of this examination are essential as a step towards the helicopter being an original design and in the context of solution methodologies. This archetypal design aims to shed light on helicopter design studies and serve as a roadmap for future research.

* Corresponding author. Department of Aeronautics and Naval Architecture, Budapest University of Technology and Economics, Muegyetem rkp. 3, Budapest H, 1111, Hungary.

E-mail address: kale.utku@kjk.bme.hu (U. Kale).

<https://doi.org/10.1016/j.heliyon.2023.e17369>

Received 30 December 2022; Received in revised form 28 April 2023; Accepted 14 June 2023

Available online 20 June 2023

2405-8440/© 2023 The Authors. Published by Elsevier Ltd. This is an open access article under the CC BY-NC-ND license (<http://creativecommons.org/licenses/by-nc-nd/4.0/>).

1. Introduction

In the developing and changing aviation industry, design is a concept that affects the entire vital process of aircraft, from performance to production [1]. In aviation especially, which has become a fundamental concept today, it is necessary to pay attention to many parameters in order to design an environmentally friendly system [2] by ensuring sustainability [3]. Additionally, it is crucial to produce an environmentally friendly solution as well as an ergonomic one [4]. Therefore, helicopter design is a vital process that must be undertaken considering many different parameters [5]. There are numerous advantages and disadvantages of using helicopter-class vehicles, a serious study in the aviation industry, and the design processes need to be conducted meticulously [6]. Among these advantages, helicopters do not need a runway under take-off and landing conditions. Moreover, helicopter systems are used for search, rescue, and transportation purposes even in the most difficult of terrain conditions [7]. These vehicles have the disadvantage of being unable to fly at high altitudes or high speeds. Considering these advantages and disadvantages, a design study should be conducted in terms of sustainability.

In this study, the preliminary design of a light-class helicopter, considering ergonomics, environment, and sustainability factors, is detailed. The planned work process, design requirements, and calculations were supported by considering the design and task requirements, based on various approaches. Within the scope of the process, the needs of the sector in helicopter design were discussed by giving importance to the literature studies. Investigating deficiencies and errors in helicopter systems, the cause of many accidents are experienced every year, the system and design criteria that should be added were also determined in this research.

Various improvements in terms of design are required for helicopter accidents, which occur in excess of 100 worldwide every year. Within the scope of design, the helicopter crashworthiness and survivability analysis study conducted by Purdue University [8] in 2016 was examined, and solutions were developed to minimize the possibility of errors and accidents in the system. In this study, it was concluded that accidents frequently occur due to obstacle impact, resonance, weather conditions, and visibility. As a solution to these, solutions such as a cockpit design with optimum visibility and the addition of dampers to the landing gear to reduce ground resonance are considered within the scope of the design. In addition, it can be mentioned that it is also important to make predictions about software reliability [9] and studies on software detection in datasets [10] in order to minimize the possibility of errors and accidents in the system.

In the structure of the study, a design methodology has been determined based on the research in the literature, and an environmentally friendly light-class general-purpose helicopter design, which is verified by performance analyses, has been put forward by adhering to this methodology. The optimum design in terms of performance, cost, and environmental features is determined by comparing it with similar products identified in the literature. The study concluded with theoretical calculations and methodology to determine the innovative features of the design.

2. Design methodology

2.1. Design requirements

The basis of the design was to produce a high-speed, environmentally friendly, and sustainable utility helicopter that would complete the determined mission profile in the shortest possible time, with low procurement and operating costs. The cockpit design for a pilot and four passengers specified in the job description was designed at an optimum volume based on anthropometric data. In the helicopter study, the design was made by considering reliability, manufacturability, environmentalism, energy consumption

Table 1

Requirements matrix: Design parameters, impact rate, requirements, and the part where these parameters are examined in the research.

Design Parameters	Effect Rate	Requirements
Sustainability	10	The most environmentally friendly propulsion system design is prioritized.
Weight	8	Since the effect of weight is encountered at many stages of the design, it is aimed to obtain minimum weight.
Manufacturability	6	In order to be competitive for the archetypal helicopter, the choice of parts and elements that cannot be produced have been avoided.
Vibration	6	Active and passive systems are integrated into the design in order to minimize vibrations to the structures and systems.
Noise	7	Compliance of the archetypal helicopter with CS-36 certification standards has been observed.
Originality	6	The design should be original and offer new solutions to the industry.
Autorotation	6	Design requirements have been considered in order to perform a safe landing in failure situations.
Stability	6	Stability and stability control have been carried out in order to ensure that the helicopter is statically and dynamically stable.
Cost	5	Production and operating costs are considered for the design in order to create a competitive product.
Structural strength	6	Maintaining the structural integrity of the helicopter is considered during the design phases.
Range	7	High range performance is aimed at without air refueling.
Endurance	7	The helicopter must have high endurance efficiency.
Mission altitude	7	Altitude values that meet the intended mission requirements must be achieved.
Innovative technology	7	The capability of design should be increased with innovative technologies.
High speed	6	The aircraft must have a high cruise speed relative to its competitors
Total	100	

reduction, innovative technology, and sustainability. An archetypal helicopter’s design work has been put forward within the determined requirements. In addition to the determined mission profile and requirements, additional requirements were created within the framework of the design in order to obtain a unique, innovative, and high-performance helicopter. Depending on these requirements, a requirement matrix was created, and the impact ratios of the requirements have been determined (Table 1).

Helicopter design work is a process in which all parameters should be examined together, considering multi-disciplinary management. However, the impact rates depending on the requirement matrix created are effective in determining the methodology and points that required importance within the scope of the study [11]. As a part of archetypal helicopter design work, a design methodology is created to proceed in a systematic and planned manner, and the design study is carried out by adhering to the methodology. In the context of the design methodology shown in Fig. 1, configuration choices depending on the various requirements were determined by the decision matrices generated.

Helicopter sizing was conducted depending on the design variables, requirements, and configuration, and performance calculations were started with consideration of various aerodynamic parameters. At the point where it converged to the estimated weight value at first, evaluation steps such as vibration, noise, and cost were started at the design stage. While paying attention to these parameters, it was considered that the design is made for an environmentally friendly and sustainable light-class helicopter. It can be said that the design work is a set of iterative processes. Weight and power calculations can be obtained within the scope of iterative processes. Until these values are in the expected range, the design parameters should be changed and the process of designing a helicopter should be managed by a number of different design disciplines [12].

2.2. Design configuration selections

In the designed light-class archetypal helicopter, configuration selections were made as a result of the decision matrices created among many configurations in the subsystem and design parameters. Decision matrices were created by considering the advantages and disadvantages of the configuration types. Table 2 shows the configuration and design decisions used in the final design. When the configurations are analyzed, it is seen that a fenestron-type tail was selected in order to reflect the environmentalist features of the noise emission level. In addition to this, a single-engine configuration was preferred due to cost considerations. In addition, the configurations determined within the scope of the design were determined to be competitive compared to similar helicopters in the literature. Configuration choices were verified by the design methodology, and manufacturability, suitability, and environmental

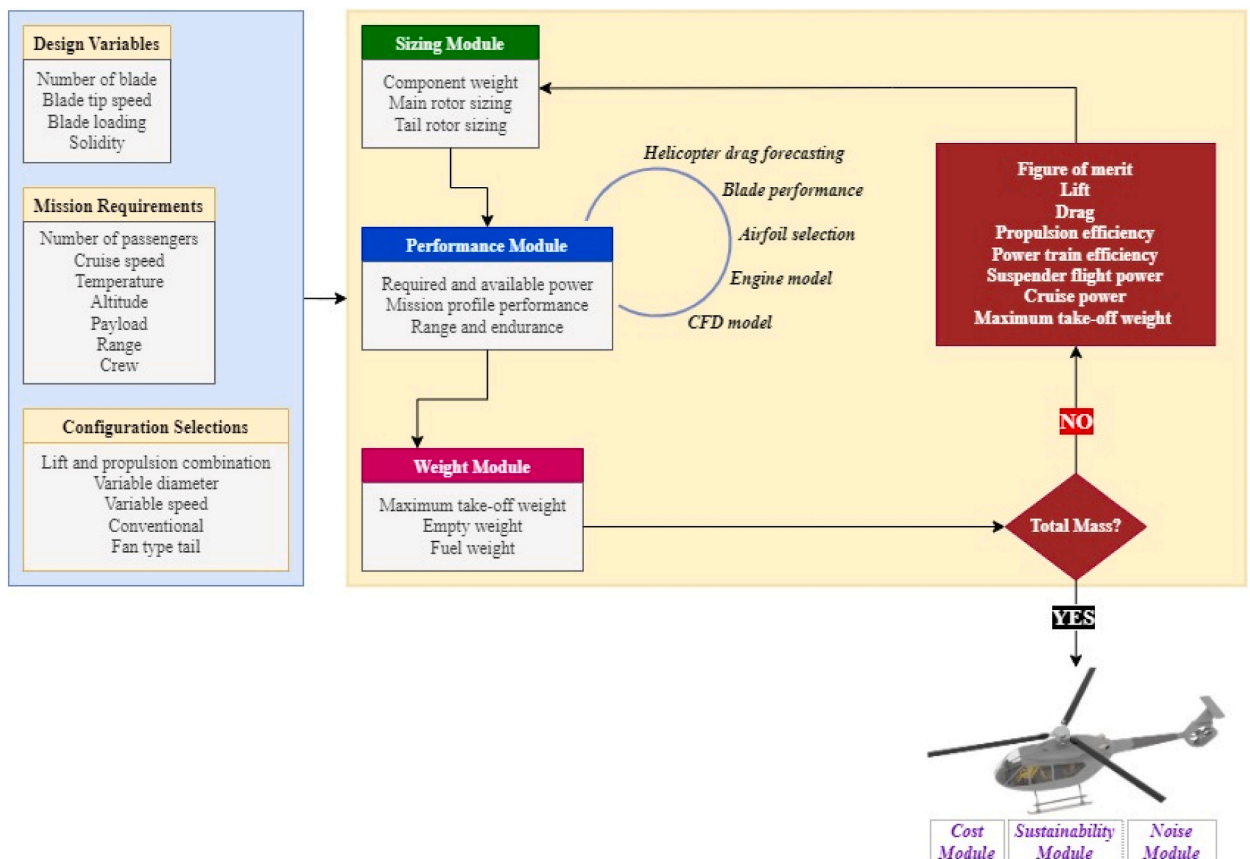


Fig. 1. Flow chart of design methodology.

Table 2
The configuration and design decisions are used in the final design.

	Design Parameters	Configurations		
Main Rotor	Main rotor type	Fully articulated	Rigid rotor	Bearingless rotor
	Blade profile	Symmetrical	Asymmetrical	
	Number of blades	2	3	4
	Engine type	Turboshaft	Electric motor	Reciprocating engine
	Number of engines	1	2	3
Tail Rotor	Tail rotor type	Conventional	Fenestron	Notar
	Blade profile	Symmetrical	Asymmetrical	
	Number of blades	4	5	6
Structural systems	Landing gear	Fixed skid	Fixed wheel	Folding wheel
	Airframe structure	Monocoque	Semi-monocoque	
Other systems	Tail type	T	H	Dihedral H
	Gearbox	Planetary gear	Helical gear	
	Control system	Hydraulic system	Fly-By-Wire	

friendliness were also taken into consideration within the scope of the selection criteria.

2.3. Performance analysis

The performance of the helicopter encompasses a set of studies covering all design processes and parameters affecting flight and operational conditions. Additionally, an accurate evaluation of helicopter design parameters and an estimation of basic flight performance in the early design stages are critical in terms of cost-effectiveness [13]. An archetypal helicopter performance analysis methodology is shown in Fig. 2. Within the scope of the established methodology, helicopter performance was examined, the necessary

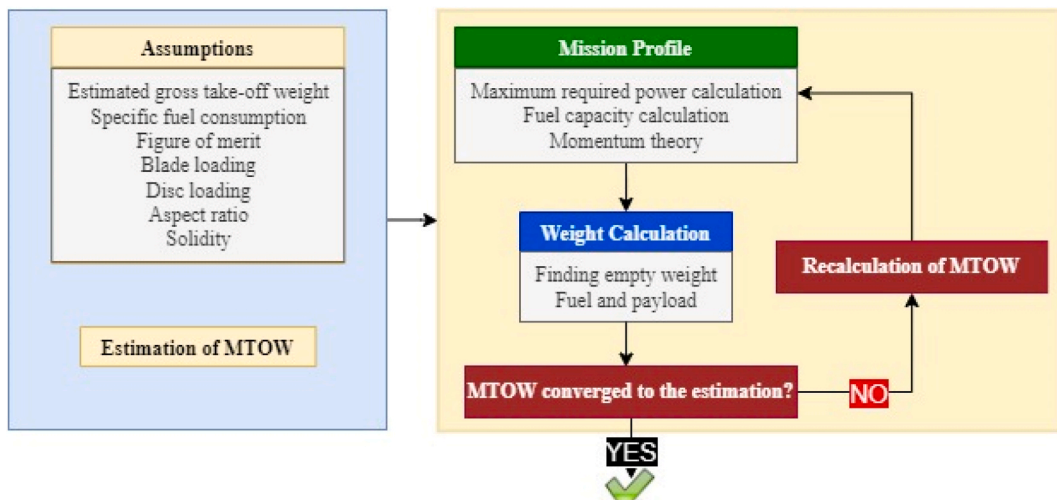














Fig. 2. Estimation of MTOW from the archetypal helicopter performance analysis.

Table 3
Benchmarking of helicopters in the light-utility class.

Specifications												
	Bell 206B3 Jet Ranger	Robinson R66	Bell 206	Enstrom 480	Eurocopter EC120 Colibri	MD Helicopters MD 500	Bell 505 Jet Ranger	Robinson R44	OH-6	Sikorsky XH-39	Schweizer S333	Archetypal
Capacity	1 + 4	1 + 4	1 + 4	1 + 4	1 + 4	2 + 3	1 + 4	2 + 3	2 + 4	1 + 3	1–3	1 + 4
Length [m]	12.09	8.99	12.09	9.09	11.52	9.93	12.93	11.66	9.24	12.5	9.5	9.33
Height [m]	2.84	3.48	2.84	2.92	3.4	2.67	3.25	3.28	2.48	2.92	3.35	3.117
Empty Weight [kg]	1057	585	1057	760	960	722	989	658	557	955	549	549
MTOW [kg]	1520	1225	1520	1293	1715	1610	1669	1134	1225	1525	1157	1287.37
Main Rotor Diameter [m]	10.16	10	10.16	9.75	10	8.33	11.28	10.01	8.03	10.67	8.38	9.7
Maximum Speed [km.h ⁻¹]	220	–	220	–	–	282	232	240	–	251	–	242.61
Cruise Speed [km.h ⁻¹]	–	200	–	211	226	250	–	200	240	222	194	222
Range [km]	693	650	693	700	727	430	617	560	610	450	591	662
Service Ceiling [m]	4100	4300	4100	3962	5180	5700	5670	–	4800	5500	–	6067
Rate of Climb [m.s ⁻¹]	6.9	5.1	6.9	7.62	6.1	10.5	–	–	10.50	–	7.0	7.37

acceptance and iterative processes were determined, and performance analysis methods were developed.

The performance review methodology covers solidity which is initialized by accepting the values of aspect ratio, disc loading, blade loading, the figure of merit, maximum take-off weight (MTOW), and specific fuel consumption (SFC) [14]. After the maximum required power and fuel capacity calculation steps based on the mission profile, and using the momentum theory, the weight value calculation is performed. Various iteration processes are applied until the calculation converges to the estimation. Parameters such as power obtained after convergence, range, rate of climb, airtime, fuel consumption, and altitude values constitute the performance parameters of the archetypal helicopter. Additionally, stability analyses, noise emissions levels, and vibration analyses performed in the follow-up of the helicopter's design processes are included in the performance analysis processes. The performance analysis processes, which are iterative methods, are continued until they meet the requirements [15]. For example, an unstable helicopter design involves rewinding and optimizing the design processes.

2.4. Benchmarking of current products

During the design process, helicopters close to the mission requirements in terms of weight and performance parameters are determined. This determination sheds light on the statistical methods used in the design study. Weight, geometric dimensions, and performance parameters obtained as a result of the design should be compared with the helicopter specifications gathered from the literature. This comparison determines the positives and negatives within the scope of competitor product analysis. The helicopters gathered from the literature research and the characteristics of the archetypal helicopter obtained as a result of the design study are shown in Table 3. When archetypal helicopter and rival helicopters are examined, it can be seen that the archetypal helicopter is lighter in weight with the same passenger capacity. The performance parameters provide an advantage over competing helicopters, revealing the various advantages (being manufacturable, environmentally friendly, and sustainable) and uniqueness of this design. The fact that the geometric parameters are larger than rival helicopters provides certain advantages and disadvantages. On the plus side, an increase in passenger comfort can be advantageous but an increased drag force can be a disadvantage. However, within the scope of the design study, the aim was to consider these advantages and disadvantages in a balanced way and to observe the optimum situation. During a review of competing products, it was also found that the offered design is better because it has more innovative technology, low production costs, as well as less noise and vibration.

3. The selection and design of subsystems

Many sub-systems need consideration, due to the helicopter's structure and in order to perform its operations. These sub-systems not only add structure to the helicopter but also enable it to be evaluated in the qualified helicopter class [16]. The sub-systems were examined under the headings of power transmission systems, control-avionics systems, rotor systems, propulsion systems, structural systems, and others. The volumes and locations of the subsystems are explained in detail.

3.1. Power transmission system

The power transmission system of the archetypal helicopter consists of a shaft, gears, bearings, clutch, brake system, and lubrication system. In the designed helicopter, the engine and the power transmission system connected to the engine were positioned at the top of the helicopter. The goal is to design the power transmission system to be as light as possible by keeping the distance between the engine and the blades as short as possible, in line with the aims of being cost-effective and environmentally friendly [17]. In the helicopter design process, the effects of power transmission elements on torsional vibrations due to vibrations created by the engine and blade systems were investigated. The main rotor power transmission system consists of various gear structures. A bevel gear reduction was used in the first stage of the main rotor power transmission system. For the second stage, both bevel gears and planetary gears were preferred. The main advantage of planetary gears is that multiple contact positions separate a large torque, resulting in an efficient and more compact speed reduction. This also enables the use of higher reduction ratios of about 5:1 that are not easily achieved with other gear configurations. Gears are made of AISI 9310 high strength gear steel and gearboxes were planned to be manufactured from magnesium due to its ability to dampen vibration. The main rotor shaft was designed to handle dynamic and static loads. Additionally, it was planned to manufacture the main rotor shaft from titanium 6Al-4V material. The powertrain reduces the engine's speed from approximately 435 rpm to 23 162 rpm [14]. These rotational speeds were given for the hover condition. For the tail rotor, an electric tail rotor configuration was preferred over the conventional tail rotor. This configuration eliminated all of the traditional mechanical anti-torque components such as gearboxes, driveshaft, and tail rotor hubs and was replaced by an electric motor and fan. Since most of the power would be transferred to the main rotor, efficiency will be achieved in terms of performance, and since there is no shaft between the stern and the engine, the negative effects of torsional force are avoided.

3.2. Control and avionics systems

The purpose of control and avionics systems was to design a modern and ergonomic system to provide the pilot with the ability to control the helicopter, maximize the design in terms of technology, and improve flight and mission capabilities [18]. It was planned to achieve these goals in the design process by integrating modern sensors, flight displays, and control architecture, which would provide greater control authority and minimize pilot workload. While doing this, the cost, weight, required maintenance cost, sustainability, and reliability parameters were considered. The central control computer, which was planned to be used in the archetypal helicopter,

is a mission computer that provides management of avionics systems in a single center. This reduces the pilot's workload by supporting the pilot with an advanced processing capability in the execution of the tasks. The structural integrity and usage tracking system planned to be implemented in the archetypal helicopter was a sensor-based monitoring system that monitors and controls the performance of critical components of the helicopter. This prevents accident risks by detecting mechanical failures before they turn into catastrophic failures. The avionics activation and display control panel planned for use in the archetypal helicopter was an avionics control panel designed for barometric adjustment, route selection, radar height adjustment, reset and emergency transmitter activation, emergency communication, and emergency communication functions. The air inertial navigation system planned for use in the archetypal helicopter was a navigation class fiberoptic gyroscope air inertial navigation system with an embedded global positioning system receiver. It continuously provides the linear acceleration, linear and angular velocity, position, and orientation information to the system it is on.

Active matrix liquid crystal display (AMLCD) technology was used in the design of the VMFD-810 multifunctional central cockpit display. It has various features such as a digital video input display, digital input/output processing, compatibility with mission computers, high resolution, compact design, ease of integration, configurable bezel keys, horizontal/vertical screen selection, wide illumination range, and wide viewing angle. The system was used as a cockpit screen in the designed archetypal helicopter. The helicopter was equipped with a weather radar for all-terrain and navigational maps. In the designed archetypal helicopter, the radar was placed on the nose of the helicopter fuselage. DHS-300 is an analog intercom system which provides the management of the radios, receivers, and audio warning devices on the helicopter and the communication interface with the pilot and co-pilot. It meets the voice communication needs of users in noisy environments in a high-quality and reliable manner digitally. This was therefore used for the communication system in the archetypal helicopter. It was decided to use the Helicopter Obstacle Detection System (HETS) as the anti-collision system. The Active HETS system, which operates in different bands, with high efficiency, high beam quality, and indifferent power ranges, is a system that ensures that warnings are given to the pilots at the appropriate time in case of a potential collisions with an obstacle, which is a common cause of helicopter crashes. In the archetypal helicopter, this system was used to minimize accidents and damage. The fuel hydraulic gauge used in the archetypal helicopter provides information to the pilot regarding the amount of fuel in the tank, hydraulic pressure, and fuel balance status. It has features such as being suitable for mission computers and easy integration.

The archetypal helicopter has features such as a display of engine parameters, a compact design with its power source, compatibility with mission computer applications, and easy integration. The Autopilot Control Panel used in the archetypal helicopter provides an operator interface for the upper functions of the autopilot system. Apart from the large set of upper functions, it also provides a head angle and height presetting capabilities. The operator interface design was designed in accordance with the "MIL-HDBK-1472 F Human Factor Engineering" standard. During the helicopter's flight and operational stages, the pilot needs to read numerous parameters (direction, pressure, temperature, and others) in the cockpit ergonomically. Therefore, the pilot can observe these parameters with the help of indicators located in the cockpit [19]. In the archetypal helicopter design, flight aid indicators were used in the cockpit to increase the safety of flight operations. Instruments found in the cockpit configuration are the following: an audio control panel; NAV/COMM, avionics specified by JAR-27 standards (magnetic compass, altimeter, and airspeed indicator), artificial horizon indicator; fuel gauge; fuel pressure gauge; transmission oil temperature, and pressure gauges; engine oil temperature, and pressure gauges; turbine gas temperature gauge, gas generator tachometer; rotor/turbine tachometer; torque meter; outdoor temperature gauge; ammeter/voltmeter; a 3-way intercom (pilot, copilot, and crew) intercom with earphone connection; fan-assisted ventilation; and heater/anti-fog and ceiling light. In helicopter design architecture, flight information is provided to the pilot from the main flight screen. Additionally, there are discrete displays for relevant parameters in the cockpit to show the data of the helicopter systems [19]. All indicators receive data from the relevant sensors by direct connection. Communication and navigation radios are operated by way of a control unit in the cockpit. In addition, there is a backup flight indicator in the cockpit to be used in emergencies, which receives and displays data from sensors completely independent of the helicopter's main systems [20]. Flight control systems are systems in which the pilot controls the helicopter rotor. It has three different control inputs: collective, cyclical, and counter-torque. The collective check is located on the left side of the pilot's seat. The rotary control arm rises from under the front of the pilot's seat.

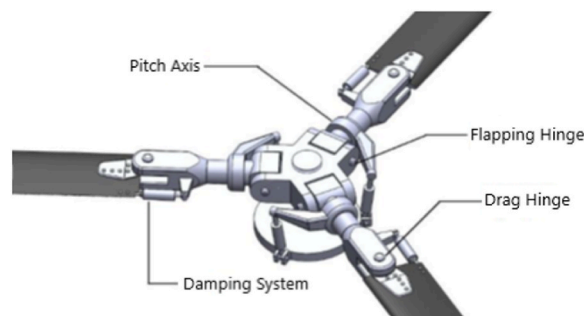


Fig. 3. Fully articulated rotor system.

3.3. Rotor systems

The main rotor system consists of a 3-blade fully articulated rotor with an SC-1095 airfoil providing excellent lift/drag ratio and high lift force (Fig. 3). In the fully articulated rotor system, a number of hinges and bearings allow the blades to move in all three axes. Each rotor blade is connected to the rotor hub by a series of hinges that allow the blade to move independently of the others. The blades make pitch movements around the longitudinal axis, forward-backward movement within the rotational plane, and flutter up and down perpendicular to the rotational plane. Therefore, the helicopter has high maneuverability and a good control response [21]. The shaft is positioned in the upper part of the body in order that the center of gravity is in line with the vertical axis.

Helicopter blades are one of the components of the helicopter that affect its helicopter's fuel consumption, emissions, sustainability, and performance in landing, take-off, and all other flight steps. A design methodology that considers high performance, efficiency, durability, and low acoustics was used in the design of helicopter blades. Within the scope of the blade design study, a basic blade geometry was created using the SC-1095 airfoil. The designed blade geometry was studied aerodynamically within the boundary conditions depending on the design and task requirements. The pressure loads along the blade were discovered as a result of this examination, and the data obtained here are used in the structural analysis. Along with the structural investigation, deformation and equivalent Von Mises stresses are determined depending on the compressive loads and boundary conditions [22]. A pre-stressed modal analysis study was carried out using these stress values. The frequency values were found by examining the modal analysis study in six modes. Since weight is an important concept in helicopter systems, material selection criteria consist of certain parameters such as lightness and strength [23]. Materials such as aluminum, composites, and titanium were used in the design of the blade (Fig. 4). The blade surface was determined as carbon fiber composite.

Vibration is one structural condition that helicopter systems are most exposed to. If vibration control is not provided, the helicopter will be subjected to a serious vibration load and damage from take-off. Since the ground resonance location situation is a dynamic instability situation, the plan is to use various dampers for vibration and ground resonance control in the helicopter system. An example of these dampers is the lead-lag damping system [22]. In terms of the innovative technology of the designed helicopter system, the vibration damping system mainly includes active systems. It was intended to dampen vibrations together with the actuators. Additionally, the aim was to reduce the vibration frequency with the optimizations made depending on the vibration values in the blade design methodology.

A fan-type anti-torque system was designed for the helicopter, as it provides safety in flights close to the ground, saves fuel by requiring less power in level flights, and provides high maneuverability for the aircraft. The main components of the fan type design are the duct (inlet port, core, stator, and diffuser) fan, and horizontal and vertical tails. An electric motor was preferred in the helicopter, as in the Bell Reveals 429. In this way, weight saving was achieved by not using the tail rotor drive shaft and gears, making it possible to design greener rotorcraft by saving weight and reducing fuel consumption. The main reasons for choosing this system are that it costs less, is faster than a shaft tail rotor, has fewer mechanical parts, and is significantly quieter. The advantages of this system are that it mitigates carbon emissions, reduces fuel consumption, and reduces the maintenance needs of the aircraft thanks to there being fewer mechanical parts. Additionally, most ground crashes in helicopters are caused by the tail rotor, which rotates much faster than the main rotor. This configuration, which has more controllability, was aimed at reducing the probability of accidents. A brushless DC motor was used for the motor. Brushless DC motors work with direct current and it converts alternating current into direct current, which is supplied to the electric motor of the tail rotor. A reasonable power-to-weight ratio value for an electric motor for general aviation rules is between six and eight kW/kg. The driving power required for the electric motors is provided by batteries (Fig. 5). For this reason, lithium-ion batteries were preferred since they exhibit high energy density and high energy efficiency compared to other batteries [24].

3.4. Propulsion system

In this step, the greener helicopter's engine selection, the air intake into the engine system, exhaust designs, and selection criteria were determined. For the engine selection, the required power values had to be found in the helicopter design process [25]. As a result of the power calculations made before the engine selection, it was determined that the power required for the helicopter's 1219 m (4000 ft) operating altitude is 317 hp and the required power for operation at sea level is 326 hp. Based on these power calculations, turboshaft helicopter engines with similar power values were determined. With the decision matrix created, engine selection was performed, considering the advantages and disadvantages. In the decision matrix, the model, power value, weight, and specific fuel

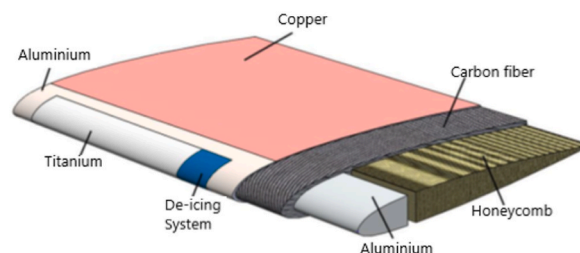


Fig. 4. The materials used in the blade design and their application section.

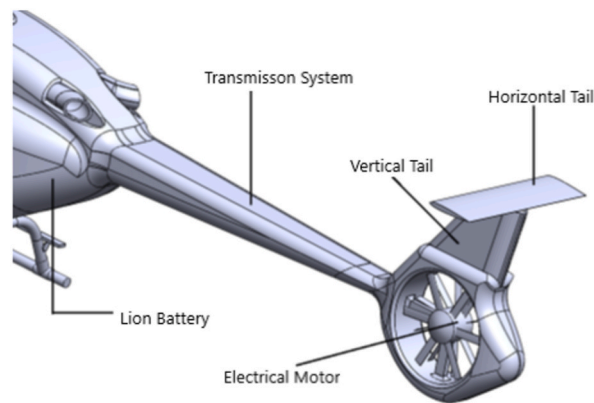


Fig. 5. Tail unit and electric motor configuration.

consumption were considered. As a result of the selection, it was decided that the most suitable engine is the Rolls-Royce C20J [18]. The weight of this selected engine is 73 kg (161 lb), its take-off power is 420 hp, and the specific fuel consumption is $0.65 \text{ lbm. lbs.hr}^{-1}$. The fact that both the engine weight and the specific fuel value of this engine are at an extremely optimum level compared to their counterparts of similar power puts the helicopter in an advantageous position in terms of weight and is also environmentally friendly.

The air intake serves to provide the engine with sufficient flow and regular airflow with low-pressure loss under all altitude and temperature conditions. This structure provides air circulation in the engine area as well as the air required by the engine. There are two air intakes in total in the helicopter. The air intake is designed as an elliptical to draw air into the chamber with a smoother transition [26]. The air intake is located so that it coincides with the natural flow lines that occur along the hull. At the same time, it will prevent foreign objects that may come from outside from entering the helicopter by locating them on the upper parts of the helicopter. The exhausts, on the other hand, are located at an angle of 30° to the helicopter's longitudinal axis, so that the flow from the engines does not affect the composite tail or main rotor blades [27]. At the same time, not to be affected by the downwash caused by the rotor, it was rotated 15° around its central axis, and with air bring directed slightly more upwards. Sand filters were installed in the exhaust system to prevent outside particles from entering the engine and causing damage. Two pieces of exhaust evacuating structures were used in the helicopter (Fig. 6).

3.5. Structural systems

The designed archetypal helicopter was structurally robust with a wide design to allow high maneuverability and operational capability. The structure was semi-monocoque, consisting of the main partition, beam, and support elements. In the archetypal helicopter, the aim should be to protect the structure and sustainability by transferring loads coming from the engine during the flight operation and the reaction forces coming from the ground during the landing operations to the fuselage. In the body design, the system strength was increased by defining the load paths within the semi-monocoque structure. Additionally, the aim was to meet the loads, such as wind and pressure, that may occur on the tail side of the fuselage by way of the load paths. The load paths are shown in Fig. 7.

The body structure was kept wide for the pilot and passenger compartments, and an ergonomic design was provided with comfort monitoring (Fig. 8). The structure was designed to minimize vibration loads that may be applied to the body. Within the scope of the design, the semi-monocoque structure design increased the strength and was evaluated according to the load criteria such as bending, tension, and compression. In addition, the body structure was designed to withstand two G's of force in 60-degree rotation operations within the scope of FAA certification. Since the tail structure is of fan type, a circular cage system was created while designing the tail. Additionally, the tail rod, which provides the tail and body connection, was designed as a truss system to minimize any errors that may arise from the transmission. The tail bar, which consists of three main compartment structures in the tail structure, consists of longitudinal beams connected to the body's main load-bearing element to increase strength. This structure was an effective tool for the helicopter to be light and durable. To mount the engine system to the helicopter fuselage, thin beams and a cage structure were formed on the upper structure of the fuselage. This structure was important for the transmission of loads coming from the engine by hosting the

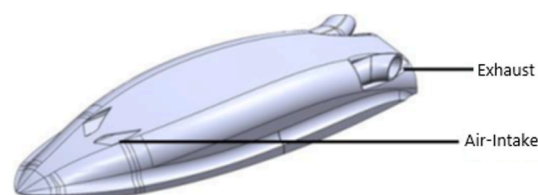


Fig. 6. The locations of the air-intake and the exhaust.

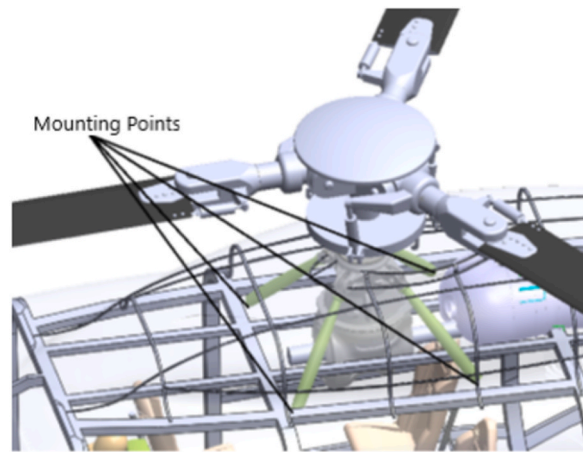


Fig. 7. Illustrative representation of load paths and mounting points.

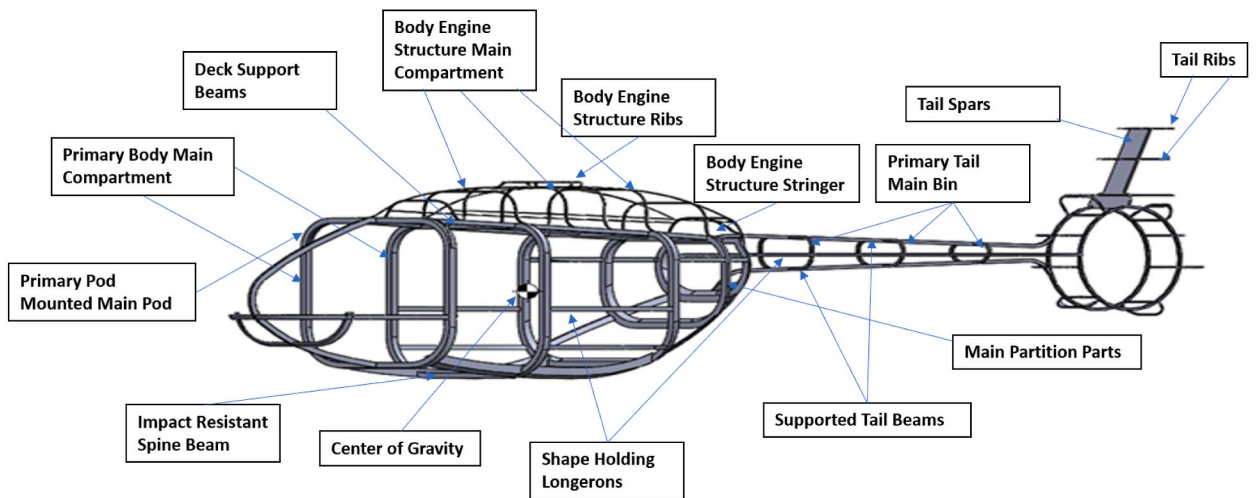


Fig. 8. The body structure of the archetypal helicopter.

engine system.

While choosing the landing gear configuration, a choice was made by creating a decision matrix that includes wheeled and skid-type configurations. Considering the dimensions and structure of the helicopter, it was seen that the skid-type landing gear gave the most efficient results. The advantages of skid-type landing gear are that it is mechanically simple in design, lighter in weight, less costly, and requires less maintenance. Considering the concept of functionality, the landing gear design was made to adapt to safety and structural demands. Under the skid tubes, there were wear plates that can be replaced to protect the load-bearing tubes from damage (Fig. 9).

Computer-aided design was used to conduct a Landing Gear Total Deformation Analysis and a Landing Gear Equivalent Strain

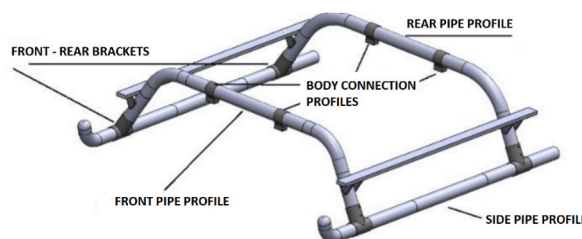


Fig. 9. Landing gear of the archetypal helicopter.

Analysis on the landing gear (Fig. 10). This indicated that the designed landing gear was good enough according to the structural limits in the CFD analysis, which are indicated by color showing minimum and maximum (Fig. 10).

The location of the ground contact points concerning the helicopter's center of gravity was chosen considering the two balance angles, the pitch and roll angles. To ensure good lateral stability of the helicopter, the roll angle should be less than 60° , and the pitch angle should be less than 30° (Fig. 11) [28].

To avoid the danger of ground resonance, the landing system must have damping elements that provide sufficient damping. The damping elements should be located between the fuselage and landing system and should ensure the stability of the system in case of possible ground resonance [29]. A number of dampers are placed on the landing gear to ensure stability. There are four elastomer insulators and four hydraulic damper cylinders in the damper slide (Fig. 12). The body damping elements used can both reduce the body frequencies and provide the necessary body damping [30]. Additional spacers were designed to connect the elastomer insulators to the skid. Therefore, it is possible to add insulators to the system without disturbing the integrity of the sled. In addition, hydraulic dampers were used to further increase the damping between the body and the skid. Hydraulic dampers were placed between the slide and the body.

Fasteners are an issue that is overlooked in helicopter design processes. However, considering the weight of the fasteners to be used during the design and the mounting and strength conditions they provide to the structure, it is necessary to examine the connection systems by adding them to the methodology in the helicopter design process [30]. Table 4 shows the difference between a conventional riveted body panel and a laser beam welded body panel. As a result of this comparison, it was decided to use laser beam welding as the connection method for joining helicopter parts due to its advantages, such as weight and low number of parts.

3.6. Cockpit, cabin, and cargo compartment

There are numerous parameters to be considered in cockpit design. One of these parameters is the anthropometric measurements of the pilot. All intended users must operate the helicopter effectively and efficiently [31]. From this point of view, a pilot's body weight of 90 kg was taken as a reference for cockpit sizing. In addition, the extensible design of the pilot seat was planned in such a way that it does not adversely affect the viewing angle, even for those of various body sizes. At the same time, ergonomic conditions were considered during the design stage of the cockpit. Maximum pilot viewing angles were provided in the cockpit design, and the front fuselage and pilot seat design was performed according to these data. Cockpit sizing according to anthropometric calculations is shown in Fig. 13, and the pilot's viewing angle is shown in Fig. 14.

There was one pilot in the cockpit and four passengers at the back, with two facing each other, in the designed light-class helicopter. To a great extent, the comfort of the passengers was also considered of importance, and ergonomic conditions were considered in the seat placements. The area behind the passenger cabin will be used as the cargo compartment. Because of the location of the fuel tanks under the cabin, it was decided to use the area behind the passenger cabin as the cargo compartment. Additionally, there are areas where passengers can put their luggage behind their seats. In the Computational Aided-Design (CAD) environment, the cargo section was designed, and the volume was found to be 0.45 m^3 .

The aerodynamic flight movements of the helicopter are provided by the flight control subsystems. Generally, cyclic, collective, and anti-torque pedals are used in helicopters. Under cyclic control, the main rotor blades move independently of each other, while at the same time the inclination angle changes of the blades are independent of each other. It is the system that provides the back and forth and lateral movement of the helicopter. Collective control, on the other hand, provides control of the inclination angles of the main

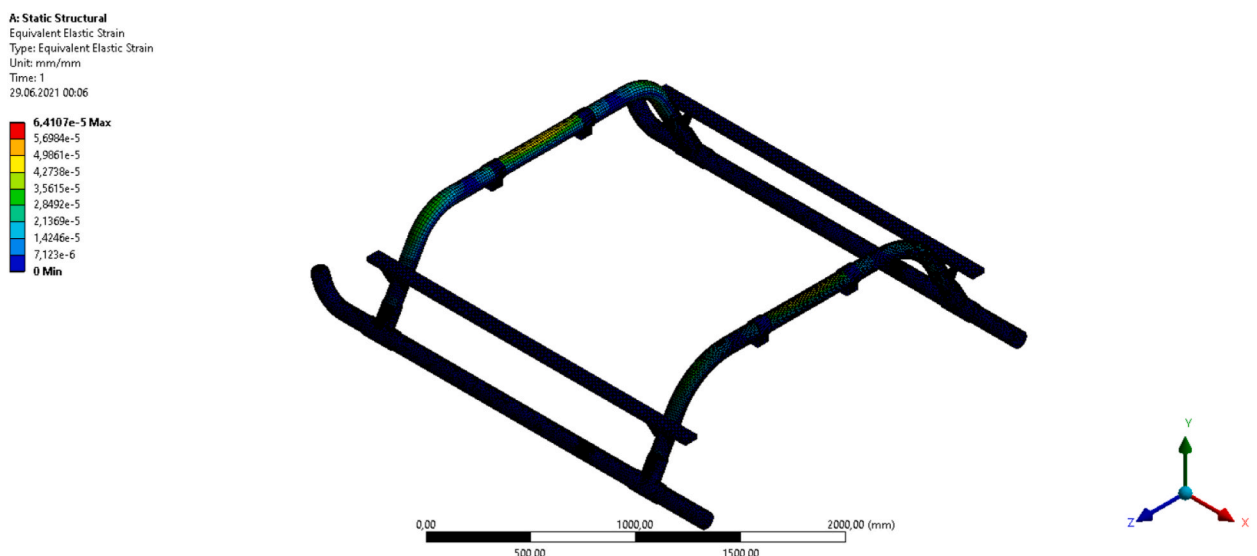


Fig. 10. Landing gear total deformation and equivalent strain analysis.

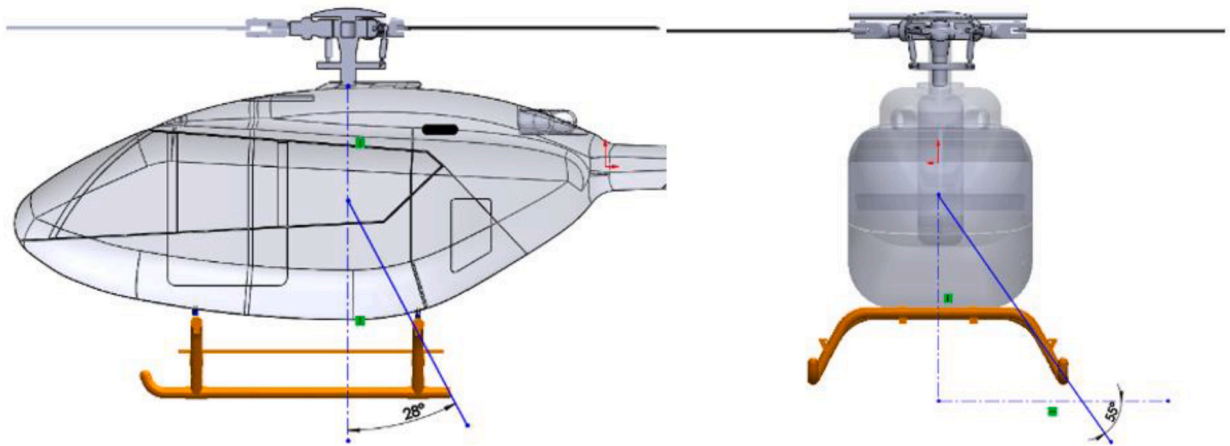


Fig. 11. The roll angle and the pitch angle of the archetypal helicopter.

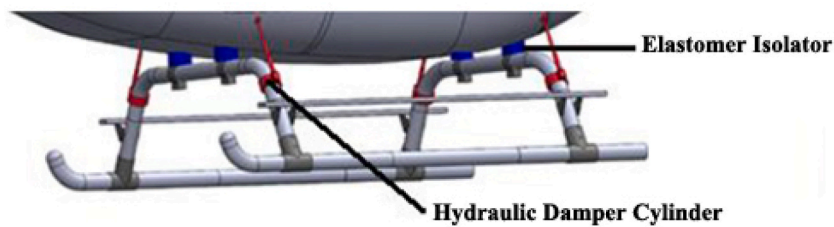


Fig. 12. The location of the elastomer isolator and hydraulic damper cylinders.

Table 4
 Benchmarking of a conventional riveted body panel and a laser beam welded body panel (Adapted from Ref. [30]).

Connection Type	Laser Beam Welding	Rivet
Advantage	Reduces the number of parts and structural complexity Lighter Works without contact No mechanical contact occurs	It is resistant to vibrations and safe There is no change in the crystal structure, therefore no distortion According to the welding, it is a more elastic connection
Disadvantage	There is no damage tolerance behavior Crack growth rates are high in heat-affected areas The initial investment cost is high	It is difficult to audit An overlay connection is possible, which aggravates the construction The rivet hole in the base material reduces the strength

rotor blades. The difference from the cyclic control is that all of the blades move together, and the tilt angles change equally. As a result, it either increases or decreases the total transport generated from the rotor [32]. The system is controlled according to the climb, descent, and level of flight performed by the helicopter. On the other hand, anti-torque pedals change the pitch of the tail rotor to increase or decrease the thrust of the tail rotor and to provide control of the helicopter in the yaw axis.

3.7. Blade profile selection

Many blade profiles can be used on the main rotor of the helicopter. Of these different blade profiles, non-symmetrical blade profiles were selected. This is because symmetrical airfoils have a low maximum lift coefficient despite having zero tilt moment. This results in a low stall margin, but this limits the maneuverability of the helicopter [33]. For these reasons, the SC 1095 airfoil was used (Fig. 15). It was thought that the selected blade profile would provide high performance. Additionally, the features of the selected blade profile are shown in Fig. 16(a-c). Fig. 16(a) presents the relation of $C_l - C_d$, while Fig. 16(b) shows $C_l/C_d - \alpha$. Moreover, Fig. 16 (c) illustrates C_p . The airfoil selection used in the tail rotor also followed the requirements. An asymmetrical blade profile with a zero inclination point in the tail profile was chosen. Care was taken to select an airfoil that would provide the highest performance values in the created airfoil pool. Within the scope of the study, it was decided that the airfoil to be used in the tail rotor would be an NACA 0012.

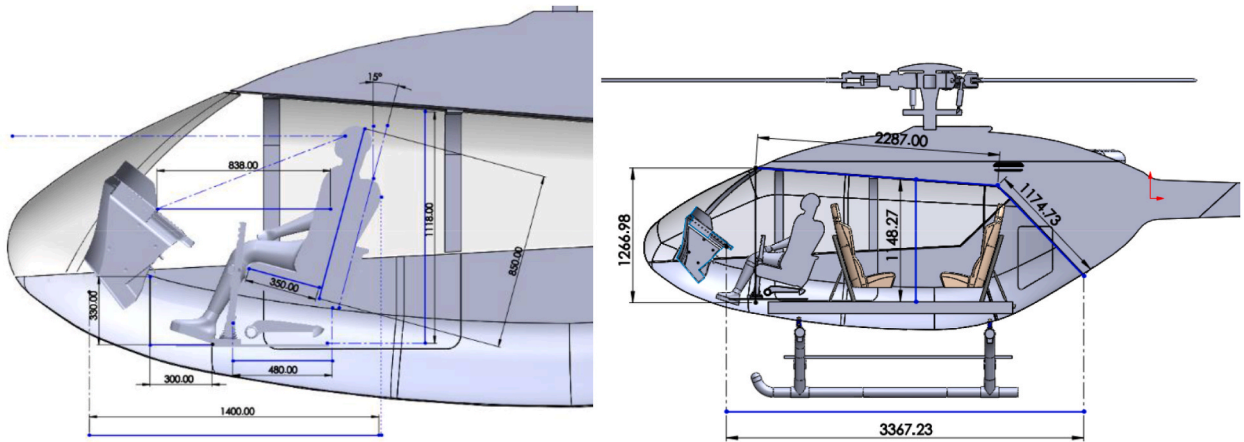


Fig. 13. The cockpit and cabin sizing according to anthropometric calculations.

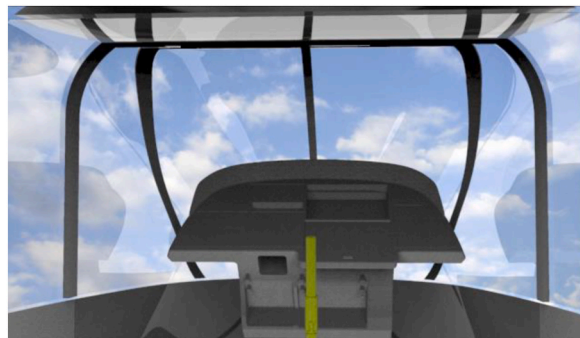


Fig. 14. The view from the pilot's eye.

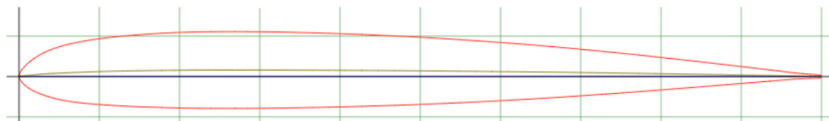


Fig. 15. SC-1095 profile ($Re = 300,000$ $M = 0.65$).

4. Performance calculations

4.1. Main rotor calculations and design

In terms of the design process for helicopters, there are a number of assumptions and optimization steps, and environmental concerns are at the forefront of this design process. One of the basic steps in starting the design process is the main rotor design (Table 5). The main parameter to be determined for the design study is the gross weight of the helicopter. Considering the design requirements, the MTOW value was determined to be 1500 kg (3307 lb). These weight estimations shed light on the weight estimation values with iterations performed depending on various parameter values in the later stages of the design process. The empty weight of the helicopter was assumed to be 60% of the initial estimated MTOW (ratio from literature) [23]. As an initial estimate, the curb weight was assumed to be 900 kg (1948.2 lb).

According to the information obtained in the literature, in the case of a helicopter hovering, the main rotor Mach number should not exceed 0.65 [34]. For this reason, the maximum type speed can be found depending on the Mach number and sound velocity parameters determined. After this, to find the rotor radius value, the disc loading value must be found. In the literature, this parameter is determined from the weight and disc loading values of similar helicopters. After this parameter is determined, the rotor radius value can be determined depending on the MTOW. According to the determined type speed and rotor radius value, the angular velocity value can be easily found. After these operations, the machete solidity value should be found. This value changes depending on the thrust coefficient and blade loading values. The thrust coefficient value depends on certain parameters such as thrust, type velocity, density,

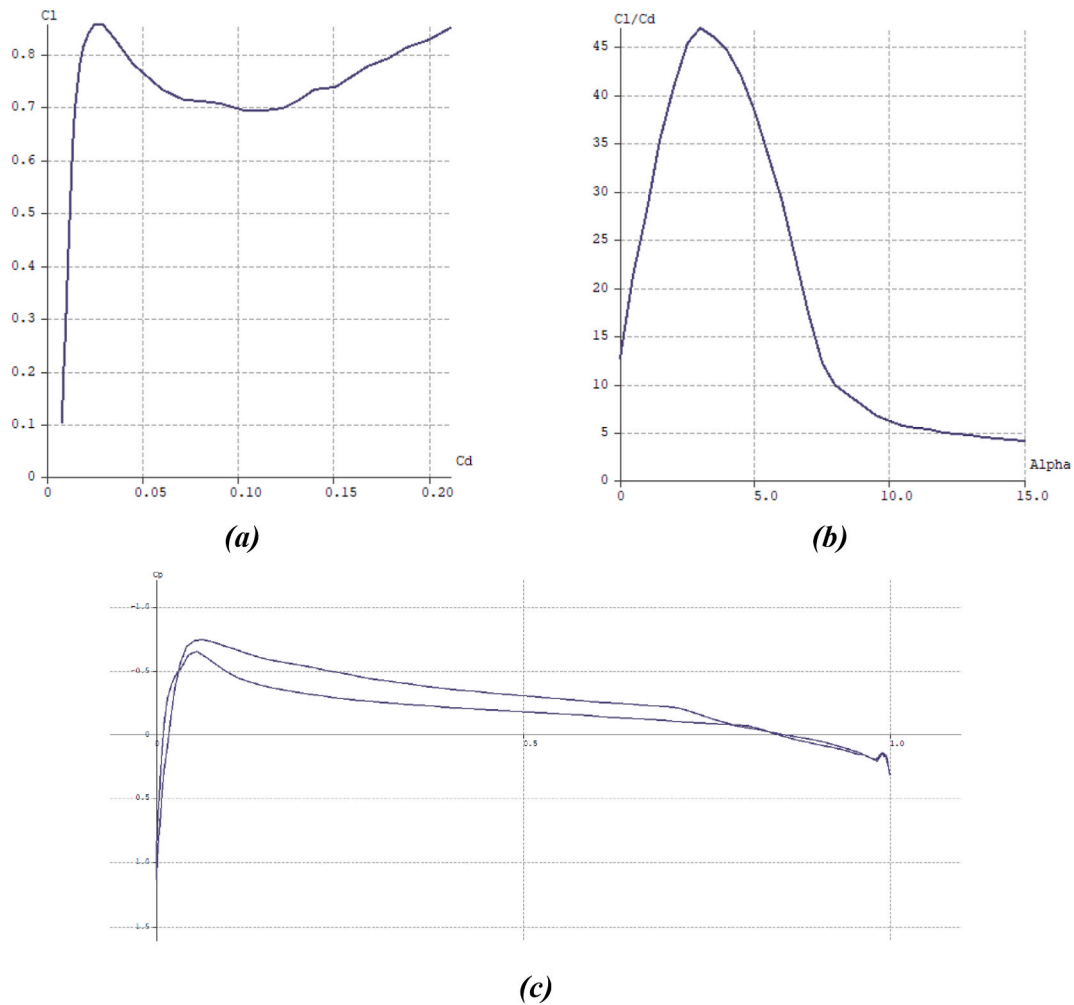


Fig. 16. The features of the selected blade profile: (a) $C_l - C_d$, (b) $C_l/C_d - \alpha$ and (c) C_p .

Table 5
Main rotor design specifications.

Parameters	SI Unit	(Imperial Units)	Values
MTOW	[kg]	[lb]	1500 (3307)
Number of Blades	N/A	N/A	3
Density	[kg. (m ³) ⁻¹]	[slug. (ft ³) ⁻¹]	1.088 (0.00211114)
Disc loading	[kg. (m ²) ⁻¹]	[lb. (ft ²) ⁻¹]	17.40 (3.5641)
Blade loading	N/A	N/A	0.067
α	[m.s ⁻¹]	[ft.s ⁻¹]	340.27 (1116.3713)
$M_{mr_{max}}$	N/A	N/A	0.65
$V_{mr_{rip}}$	[m.s ⁻¹]	[ft.s ⁻¹]	221.1755 (725.6413)
R_{mr}	[m]	[ft]	4.8527 (15.9210)
Area	[m ²]	[ft ²]	73.98 (796.3250)
$\mu_{mr_{max}}$	[rad.s ⁻¹]	[rad.s ⁻¹]	45.5770
C_{thrust}	N/A	N/A	0.0032
Blade chord	[m]	[ft]	0.2432 (0.7978)
AR	N/A	N/A	19.95
C_{lift}	N/A	N/A	0.402

and area. The blade loading range of high-speed helicopters is chosen as the initial estimate, between 0.065 and 0.07 [19]. The number of blades should be chosen at the optimum point, according to the design parameters of the helicopter. The greater the weight of the helicopter, the greater the lifting force of its blades should be. Additionally, surface areas vary depending on the number of blades. Considering all of these parameters, it was deemed appropriate to use three blades in the design. Table 5 shows the initial estimation

parameters of the main rotor.

4.2. Tail rotor calculations and design

The tail rotor produces an anti-torque force against the torque produced by the main rotor on the fuselage. It also gives the helicopter yaw stability and control in the yaw axis. Another advantage of the tail rotor is stability. For instance, if the nose is swinging to the left, the tail rotor will provide additional climbing performance [19]. The tail rotor was designed, dependent on various parameters (Table 6). The tail rotor radius is a parameter based on the MTOW. The rpm of the tail rotor is related to the rpm of the main rotor. It is accepted as approximately 4.5 times the main rotor rpm value [20]. The value of 6.5 was chosen because the tail rotor opening ratio value should be between 4.5 and 8 within the scope of the literature research. While calculating the chord value of the tail rotor, it was found to depend on the rotor radius and aperture ratio. In addition, the fan type tail was selected with the decision matrix made as the tail type mentioned earlier. Depending on this selection, the number of blades of the tail rotor was determined as six. At the command of the pilot, these six blades move angularly and define the movement in the yaw axis and the anti-torque.

4.3. Fan type tail calculations and design

The design parameters, such as high aerodynamic efficiency are aimed at the fan design. The horizontal tail is positioned above the vertical tail, preventing it from being affected by the downwash condition. The inlet lip consists of a round section that creates the suction force that allows air to be drawn. Experimental results by the United Technology Research Center (UTRC) show that a tip radius of 5–7% of the fan diameter should be present. The lip radius selected for the current configuration is 7% of the fan diameter [35]. The hub consists of fan blades and stator parts. The number of fan blades was determined as six. The stator blades help increase efficiency by reducing the eddy component downstream of the fan. The number of stator blades was obtained from the literature and taken as ten for the fan-type tail [36]. The role of the diffuser is to prevent trail narrowing, which is typical of conventional tail rotors while preventing flow separation. The diffusion angle was chosen as five, based on values suggested in the literature [37].

While designing, the appropriate fan diameter and beam were selected for a helicopter of this size by researching the literature. Design parameters such as the channel width, diffuser angle, and so on seen in Fig. 17 were later selected in accordance with the literature. High aerodynamic efficiency was the aim of the fan design. In addition, the horizontal tail was positioned on top of the vertical tail to prevent a downwash situation. A fan-type anti-torque system was designed for the helicopter, as it requires less power on straight flights, provides safety in near-ground flights, and offers high maneuverability for the aircraft.

4.4. Helicopter sizing calculations

The overall dimensioning of the helicopter should aim at it being quick, simple, and sustainable during the preliminary design work. It is necessary to use a number of quasi-experimental design tools to create a suitable configuration during the design phase [23]. One of the most commonly used tools is to perform a design trend study, based on the statistical data for existing helicopters. A literature review of similar helicopters that meet the mission requirements was conducted. It is desired to establish a design trend using the data of similar helicopters in Table 3. Overall dimensions, such as fuselage height-length, landing gear width, and tail rotor arm were determined at this stage based on statistical data. The graphics used to calculate the overall dimensions of the helicopter are shown in Fig. 18(a–c) together with the equations created. Fig. 18(a) is a graph comparing the fuselage height – main rotor diameter – fuselage length of existing helicopters and the archetypal helicopter, whilst Fig. 18(b) presents main rotor diameter – landing gear width. Moreover, Fig. 18(c) shows main rotor diameter – vertical tail arm of the archetypal helicopter.

Table 6
Tail rotor design specifications.

Parameters	SI Unit	(Imperial Unit)	Values
R_{tr}	[m]	[ft]	0.6675 (2.1901)
rpm	[rad.s ⁻¹]	[rad.s ⁻¹]	204.99
C_{d0}	N/A	N/A	0.000138
L_{CG} to tail rotor	m	ft	5.67 (18.6111)
AR_{tail}	N/A	N/A	6.5
b	N/A	N/A	6
c	N/A	N/A	0.3369
$Solidity_{tail}$	N/A	N/A	0.2938
Thrust	[kN]	[ft.lb.s ⁻²]	20.770 (4669.37)
V_{tip}	[m.s ⁻¹]	[ft.s ⁻¹]	136.9125 (449.1881)
$Area_{tail}$	[m ²]	[ft ²]	1.3999 (15.0688)
$C_{thrust-tail}$	N/A	N/A	0.0226
B	N/A	N/A	0.9646
Pi_{tr}	[kW]	[hp]	9.7429 (13.0655)
P_o	[kW]	[hp]	0.01983 (0.0266)
$PT_{tr-hover}$	[kW]	[hp]	9.7627 (13.0921)

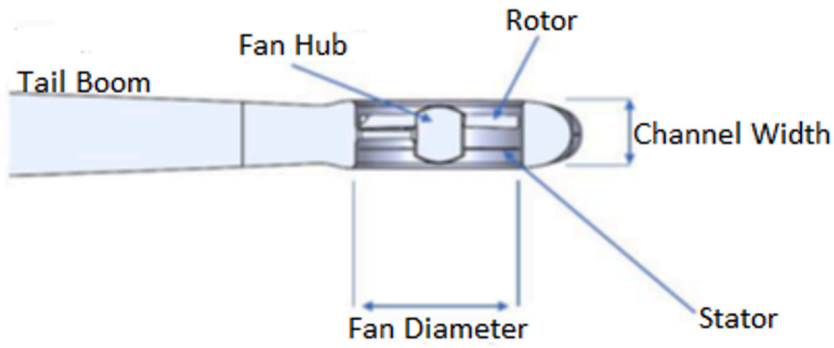


Fig. 17. Fan-type tail duct design.

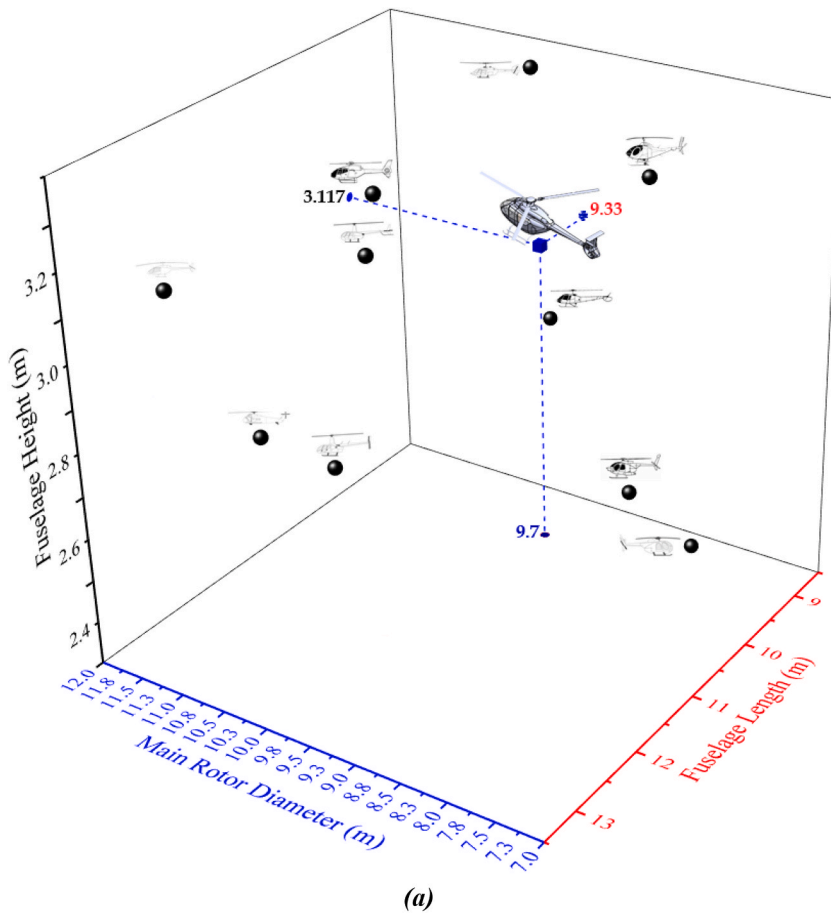


Fig. 18a. Helicopter sizing graphs; (a) fuselage height – main rotor diameter – fuselage length

4.5. Weight breakdown calculations

Various design variable parameters, depending on the determined task requirements, constitute the basic building blocks of the design [38]. Here, the design variable parameters were used in the main and tail rotor sizing calculations together with the initial weight estimation. After sizing the rotor, the power calculations of the rotors were performed, and the weight breakdowns were shown according to these power values. In this part, iterative steps were followed and the optimization process was observed. The steps of this method are shown in Table 7.

One of the factors affecting many parameters while designing a helicopter is the power calculations step. Power calculations were widely examined, and first of all, the required power value in the suspended state was estimated. According to the estimation, after the

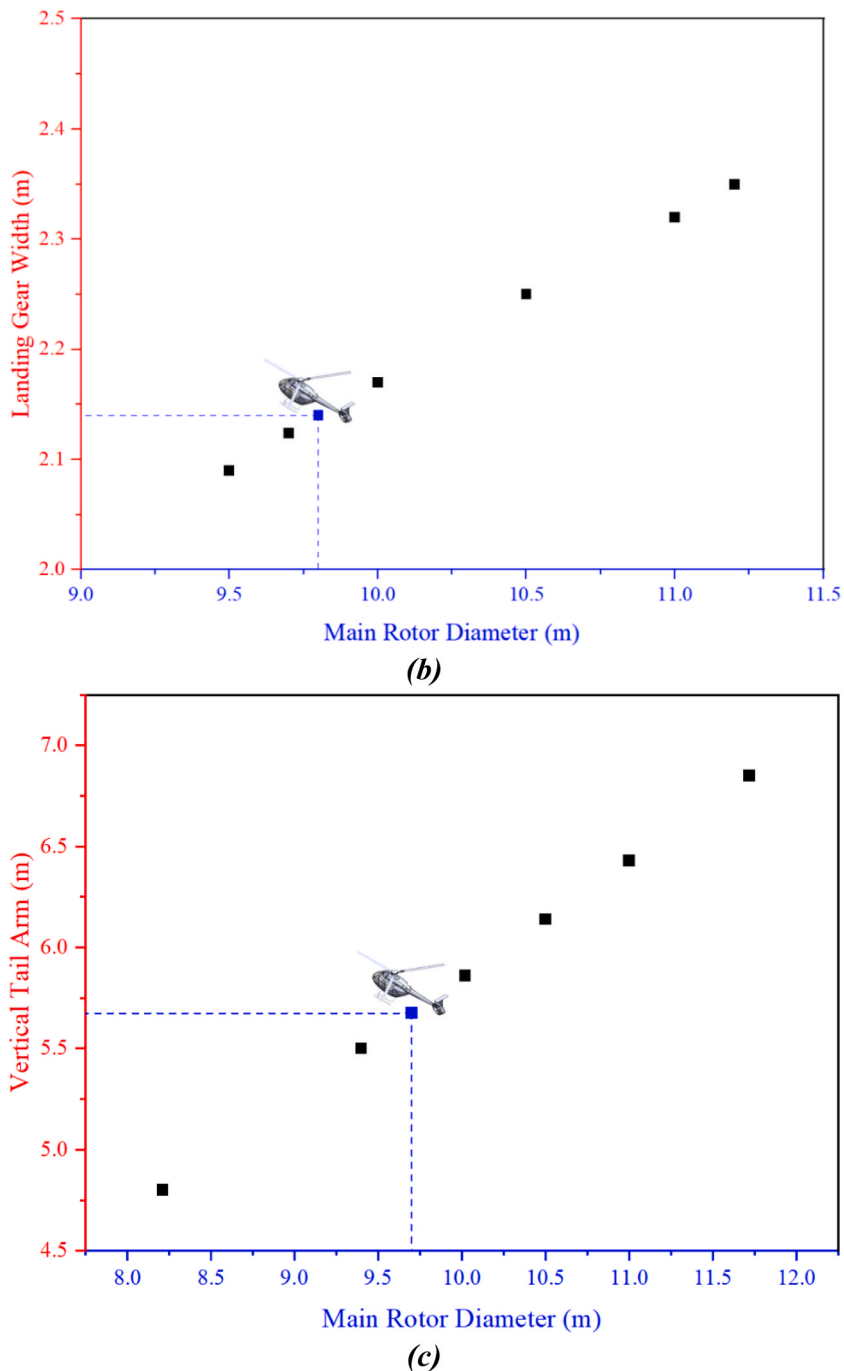


Fig. 18b. (b) main rotor diameter – landing gear width, (c) main rotor diameter – vertical tail arm.

weight iteration was concluded, the values converged to a 10% difference in the fourth iteration, and the general weight breakdown, including each subsystem of the helicopter, is shown in Table 8.

4.6. General performance calculations

At this level of helicopter performance calculations, the power coefficients are calculated for different sections in the mission profile, adhering to Leishman [34] and Johnson [19]. The total power was calculated by finding the induced power, parasitic power, profile power, and climbing power for each section from the power coefficients found.

While conducting the performance calculations, separate calculations were made for ten different task divisions: ground operation,

Table 7
Weight estimation iteration.

Parameter	SI Unit (Imperial)	1	2	3	4	5	6
Solidity _{mr}	N/A		0.0546	0.0525	0.0500	0.0479	0.0460
Blade Number	N/A		3	3	3	3	3
C _{d0-mr}	N/A		0.01	0.01	0.01	0.01	0.01
Disc Loading	[kg. (m ²) ⁻¹] [lbs. (ft ²) ⁻¹]		19.87 (4.07)	19.09 (3.91)	18.21 (3.73)	17.38 (3.56)	16.75 (3.43)
Density	[kg. (m ³) ⁻¹] [slug. (ft ³) ⁻¹]	1.088 (0.0021)	1.088 (0.0021)	1.088 (0.0021)	1.088 (0.0021)	1.088 (0.0021)	1.088 (0.0021)
α	[m.s ⁻¹] [ft.s ⁻¹]		340.27 (1116.37)	340.27 (1116.37)	340.27 (1116.37)	340.27 (1116.37)	340.27 (1116.37)
Mach Number	N/A		0.65	0.65	0.65	0.65	0.65
V _{mr,tip}	[m.s ⁻¹] [ft.s ⁻¹]	221.175 (725.64)	221.175 (725.64)	221.175 (725.64)	221.175 (725.64)	221.175 (725.64)	221.175 (725.64)
Power _{tot}	[kW] [hp]		200.52 (272.63)	190.22 (258.12)	176.15 (239.50)	164.62 (223.83)	154.94 (210.66)
R _{mr}	[m] [ft]	4.853 (15.921)	4.905 (16.092)	4.897 (16.066)	4.874 (15.991)	4.853 (15.921)	4.833 (15.858)
Area _{mr}	[m ²] [ft ²]		75.58 (813.53)	75.33 (810.87)	74.63 (803.33)	73.98 (796.32)	73.38 (789.99)
μ _{mr,max}	[rad.s ⁻¹]		45.09	45.17	45.38	45.8	45.76
C _{thrust-mr}	N/A		0.0037	0.0035	0.0034	0.0032	0.0031
Blade Loading	N/A		0.07	0.07	0.07	0.07	0.07
Blade Chord	[m] [ft]		0.28 (0.92)	0.27 (0.88)	0.26 (0.84)	0.24 (0.80)	0.23 (0.76)
AR _{mr}	N/A		17.50	18.18	19.09	19.96	20.76
W _{rotor-Blades}	[kg] [lb]		62.85 (138.55)	55.08 (121.41)	48.57 (107.08)	43.13 (95.08)	38.58 (85.06)
W _{Hub/Hinges}	[kg] [lb]		39.03 (86.04)	34.64 (76.36)	31.04 (68.43)	27.96 (61.65)	25.34 (55.87)
W _{Total}	[kg] [lb]		101.9 (224.59)	89.71 (197.77)	79.61 (175.52)	71.09 (156.73)	63.93 (140.94)
W _{Propulsion}	[kg] [lb]		148.4 (327.16)	140.5 (309.74)	130.4 (287.40)	121.8 (268.59)	114.7 (252.80)
W _{Fuselage}	[kg] [lb]		189.0 (416.68)	167.8 (370.04)	150.7 (332.30)	136.04 (299.92)	123.50 (272.27)
W _{Control}	[kg] [lb]		54.0 (119.05)	47.96 (105.73)	43.06 (94.94)	38.87 (85.69)	35.28 (77.79)
W _{Electrical}	[kg] [lb]		54.0 (119.05)	47.96 (105.73)	43.06 (94.94)	38.87 (85.69)	35.28 (77.79)
W _{Fixed-Eq}	[kg] [lb]		252.0 (555.58)	223.8 (493.39)	200.97 (443.07)	181.39 (399.89)	164.66 (363.02)
W _{Empty}	[kg] [lb]	900.02 (1984.20)	799.28 (1762.11)	717.76 (1582.40)	647.81 (1428.18)	588.09 (1296.52)	537.33 (1184.61)
W _{Fuel}	[kg] [lb]		149.7 (330)	149.7 (330)	149.7 (330)	149.7 (330)	149.7 (330)
W _{Payload}	[kg] [lb]		489.9 (1080)	489.9 (1080)	489.9 (1080)	489.9 (1080)	489.9 (1080)
W _{Gross}	[kg] [lb]	1500.03 (3307.00)	1438.85 (3172.11)	1357.33 (2992.40)	1287.37 (2838.18)	1227.66 (2706.52)	1176.90 (2594.61)

According to Mouille and D’Ambra [37], the blade loading value is that the blade loading range of high-speed helicopters, and this is chosen as the initial estimate. This value is between 0.065 and 0.07. According to this data, other parameters were included in the iteration and subsequently calculated.

Table 8
Weight estimation iteration power table.

Parameters	Units	1	2	3	4	5
B	N/A	0.9715	0.9720	0.9727	0.9733	0.9738
Pi _{mr-TL}	[kW] [hp]	134.9524 180.9742	126.91752 170.1992	116.7493 156.5635	108.2483 145.1634	101.1527 135.6480
P _{0mr}	[kW] [hp]	68.34958 91.6583	65.5616 87.9196	61.8473 82.9386	58.6599 78.6643	55.9387 75.0150
PT _{mr-hover}	[kW] [hp]	203.3021 272.6326	192.4791 258.1188	178.5967 239.5021	166.9083 223.8277	157.0914 210.6631

take-off, climb, cruise, landing, ground operation, take-off, cruise, descent, and landing. In addition, the necessary calculations for 15 min of flight at the best airspeed for the desired reserve fuel were made in the mission section.

- While calculating the power coefficients, the empirical correction factor was accepted as κ = 1.15 in the hovering flight and κ = 1.2 in the forward flight section [19,34].
- While calculating the power in the ground running sections, the engine was considered as having 7% of the maximum power that the engine can give, according to International Civil Aviation Organization (ICAO) standards, at 100% RPM rotor speed at idle.
- The total power required in hover flight, climb, descent, and level flight situations was obtained by increasing the main rotor power by approximately 10%, considering the power losses.
- Calculations have been made considering the best climb speed of 7.38 m s⁻¹ (24.2 ft s⁻¹) in the climbing and descending sections. In addition, the distances covered in the climbing and descending sections were included in the range in forward flight.

In the calculations made for each segment, the amount of fuel spent for each mission was subtracted, and a new weight was

Table 9
Task profile performance.

	Ground Operation	Take-Off	Climb	Cruise	Landing	Ground Operation	Take-Off	Cruise	Descent	Landing	Reserve
Mission Weight [kg]	N/A	1287.29	1285.03	1284.12	1210.18	N/A	809.66	808.75	757.05	756.59	755.23
[lb]		2838	2833	2831	2668		1785	1783	1669	1668	1665
Induced Power [kW]	N/A	143.92	4.47	6.31	139.29	N/A	76.06	4.26	1.7	67.11	2.16
[hp]		193	6	8.46	186.80		102	5.71	2.28	90	2.9
Profile Power [kW]	N/A	17.89	17.48	34.69	17.15	N/A	17.48	37.17	18.02	18.02	18.02
[hp]		24	23.45	46.53	23		23.45	49.85	24.17	24.17	24.17
Parasite Power [kW]	N/A	N/A	N/A	168.53	N/A	N/A	N/A	93.21	N/A	N/A	105.89
[hp]				226				125			142
Climb Power [kW]	N/A	N/A	67.86	92.89	N/A	N/A	N/A	58.16	39.52	N/A	54.44
[hp]			91	124.57				78	53		73
Total Power [kW]	21.92	161.82	90.23	302.75	156.59	21.92	93.21	213.27	59.66	93.21	199.85
[hp]	29.4	217	121	406	210	29.4	125	286	80	125	268
Fuel Consumption [kg]	1.33	2.25	1.10	73.48	0.95	0.67	0.57	51.71	0.73	1.14	9.07
[lb]	2.94	4.95	2.43	162	2.1	1.47	1.25	114	1.6	2.51	20
Distance	N/A	N/A	0.877	149.12	N/A	N/A	N/A	149.12	0.877	N/A	N/A
[km]			2877.30	489238.8				489238.8	2877.30		
Time in Mode [min]	10	2	2	35	1	5	1	35	2	2	15

calculated for the following flight segment. Weight reduction in the passenger compartment was also considered. As a result of the MATLAB code, separate power values for each task section, the distance covered, and the time spent during the task are shown in Table 9. While our estimated fuel consumption in the weight breakdown was 149.68 kg (330 lb), the fuel consumption in the mission profile calculation was 142.99 kg (315.25 lb). Calculations were continued considering that 6.8 kg (15 lb) of extra fuel was left in the tank extra as an assumption for tolerance.

Within the scope of requirements, the task profile performance was examined and performance parameters such as speed and duration, were found for all operational steps in the performance content. The performance parameters found are shown in Table 9. The helicopter's range, airtime, rate of climb, and altitude values must be included in the design calculations. These mentioned parameters are those that affect how well the helicopter works and should be considered as much as possible in the design methods.

4.7. Range and airtime

Range and airtime are mainly related to weight, power, and specific fuel consumption of the engine. For the helicopter to reach its maximum range, it must have high speed. To maximize the airtime, the helicopter must fly in the minimum power range [36]. For this reason, optimum situation monitoring should be made in in-flight operations, and the aim should be to ensure that the range and airtime are efficient. While calculating the range, the power values were recalculated after the engine selection was used. As a result of the range calculation made, the range speed was found to be 50.29 m s^{-1} (165 ft s^{-1}) for International Standard Atmosphere (ISA) standards and 357.83 nmi in ISA standards. The calculations were performed for ISA and ISA (+20 °C). The range calculation gave us a really strong advantage when the competitor analysis was conducted.

The velocity for airtime is the name given to the velocity of the Prereq curve at its minimum position when the Prereq and Available curves are plotted on the power-velocity graph. The speed at this point is the speed required at minimum power. This shows us the speed at which the system stays in the air the longest. This speed was set at 28.04 m s^{-1} (92 ft s^{-1}). In addition, the intersection point of the Prereq and Available curves on the curve shows the maximum speed of the helicopter. This value was found to be 67.67 m s^{-1} (222 ft s^{-1}) and was detailed in the attached chart. The airtime of the helicopter was a parameter related to the minimum power value and fuel weight of the helicopter. While calculating this parameter, the minimum power value in the best air retention graph was determined as 141.9 hp. When the operations related to this value and fuel load were completed, the duration of the helicopter in the air was determined as 3.7504 h by ISA standards. This value provides a convergent value in the competitor analysis, and is more than enough time to fulfill the given tasks. Figs. 19 and 20 show the results of these processes for both ISA and ISA (+20 °C).

4.8. Calculations of climb rate and altitude values

The rate of climb is a value obtained through various iterations. The maximum climb rate value at the point where the total power value calculated, according to the estimated entered climb rate value converges to the total power value calculated for the design is evaluated as a performance parameter [39]. As a result of the iteration, the maximum climb rate of the helicopter was found to be 7.37 m s^{-1} (24.2 ft s^{-1}). This value is similar to class helicopter values in the literature. In this section, the calculation of the maximum altitude values that the helicopter can reach in flight operations is shown. It is defined as the IGE altitude (in-ground effect) and is the altitude at which the ground effect exists. While finding this suspended altitude, the altitude value was decided by looking at the suspended ceiling Hovering in Ground Effect (HIGE) altitude-weight graph depending on the engine used. The IGE altitude determined separately for the ISA and ISA (+20 °C) conditions was 5200.8 m (17 063.1 ft) in the ISA condition.

The OGE altitude (out-ground effect) can be defined as the altitude without ground effect, and this altitude value was found to be 3687.6 m (12 098.6 ft) in the ISA condition. This value was discovered under the ISA (+20 °C) condition. The altitude value was determined by looking at the height-weight graph of the suspension ceiling Hovering Out of Ground Effect (HOGE). Service altitude was defined as the altitude at which the rate of climb drops to 30 m min^{-1} (100 ft min^{-1}). Under the ISA condition, this attitude was determined to be 6067.7 m (19 907.3 ft). The service ceiling value was found with the help of a service floor graph. Range and airtime calculations for the ISA and ISA (+20 °C) standards are shown in Table 10.

4.9. Autorotation calculations

Autorotation is a piloting technique that allows the helicopter to land safely in the event of a malfunction in the engine when the helicopter is in the air [40]. Under normal conditions, air flows down the rotor while it is running, but in autorotation, air flows upwards from the rotor system. Fig. 21 below shows a schematic picture of a safe landing under autorotation conditions. The helicopter enters autorotation at position 2. In position 3, it can be seen that the forward speed of the helicopter slows down and at the same time it decreases the descent rate. In position 4, the distance between the tail and the ground gradually decreases. In this state, the helicopter is brought to the horizon, and in position 5, the helicopter will have lands safely.

Overall designed helicopters must have autorotation capabilities (AI) and autorotation depends on certain parameters [34].

$$AI = \frac{I_R \Omega^2 \rho}{2WDL\rho_0} \quad (1)$$

The autorotation capability is determined from Eq. (1), the expression $I_R \Omega^2 2W^{-1}$ denotes the kinetic energy of the rotor. At the same time, according to the literature research, AI should be at least $1.25 \text{ m}^3 \text{ kg}^{-1}$ ($20 \text{ ft}^3 \cdot \text{lb}^{-1}$) in single-engine helicopters and 0.62

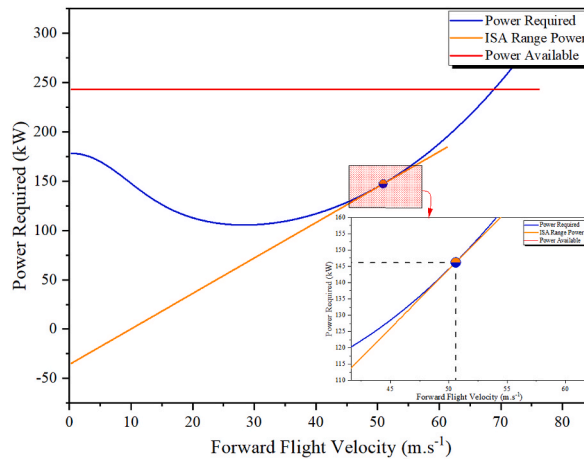


Fig. 19. The best range velocity chart under ISA conditions.

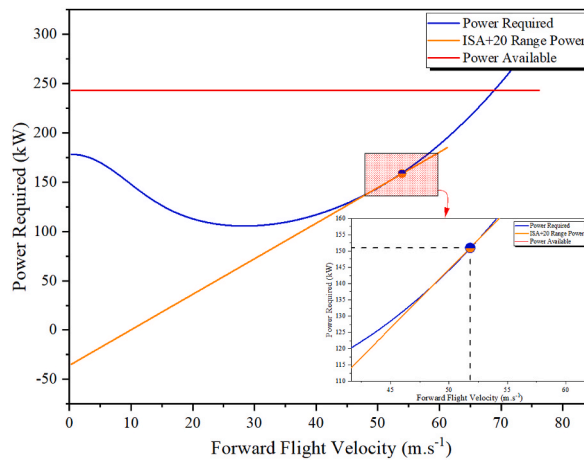


Fig. 20. The best range velocity chart at ISA (+20 °C).

$m^3 kg^{-1}$ ($10 ft^3. lb^{-1}$) in multi-engine helicopters for safe autorotation.

As can be seen in Fig. 22, there are autorotation indexes of various helicopters according to the literature research [12]. As a result of the calculations, the autorotation index of the archetypal helicopter is approximately 37. This value is sufficient for safe autorotation.

4.10. Noise emissions level calculations

Noise level should be designed at a minimal level, considering passenger comfort and the discomfort it may create. The archetypal helicopter was designed with the aim of minimum noise level during flight and operational steps.

While determining the noise level (sound pressure level, SPL), the Davidson & Hargest formula is used concerning Wayne Johnson’s [19] source. In Eq. (2), the noise value originating from the rotor is found in the hover flight condition. In the noise calculation made according to the equation, a noise value of approximately 86 dB was obtained.

$$SPL_{hover} = 10 \log \left[(wR)^6 A_b \left(\frac{C_T}{\sigma} \right)^2 \right] - 36.7 \tag{2}$$

The noise level changes depending on the number of blades. The reason for this is that air escaping from the trailing edge, depending on the gaps of the blades, creates a swirl and the following blade hits this vortex. Therefore, the noise value should be determined in the design methodology and the optimum selection criteria should be observed in the number of blades depending on the noise value. Fig. 23 shows how loud a helicopter with three blades is based on how fast the tips are moving.

The noise value obtained was examined depending on the CS-36 certification determined within the requirements. An innovative design was achieved by aiming to keep the value compared to the determined old and new limits below the limit values. Fig. 24 shows

Table 10
Range and airtime calculations.

Parameter	SI Unit	(Imperial Units)	ISA	ISA (+20 °C)
$T_{sea\ level}$	[°C]	[°R]	15 (518.67)	35 (554.67)
$T_{@4000ft}$	[°C]	[°R]	7.07 (504.41)	27.07 (540.41)
$P_{sea\ level}$	[kPa]	[Psf]	101.325 (2116.2)	106.11 (2216.2)
$P_{@4000ft}$	[kPa]	[Psf]	87.51 (1827.7)	87.70 (1831.7)
SFC	[kg.N.hr ⁻¹]	[lbm.lbs.hr ⁻¹]	0.65	1.069
ZHI α_{ave}	N/A	N/A	90	90
β	N/A	N/A	0.5	0.5
Q_{spec}	N/A	N/A	0.9725	0.9743
δ_{spec}	N/A	N/A	0.8627	0.8637
ZHI	N/A	N/A	76.6542	76.7245
P_{SHP}	[kW]	[hp]	114.32 (153.31)	114.43 (153.45)
Max Speed	[m.s ⁻¹]	[ft.s ⁻¹]	67.67 (222)	67.67 (222)
Range Velocity	[m.s ⁻¹]	[ft.s ⁻¹]	50.29 (165)	51.82 (170)
Endurance Velocity	[m.s ⁻¹]	[ft.s ⁻¹]	28.04 (92)	28.04 (92)
$RSHP_{Req-end}$	[kW]	[hp]	220.13 (295.21)	220.24 (295.35)
$V_{f_{end}}$	[m.s ⁻¹]	[ft.s ⁻¹]	44.99 (147.6042)	44.99 (147.6042)
$RSHP_{Req-cruise}$	[kW]	[hp]	273.9 (367.31)	274 (367.45)
$V_{f_{cruise}}$	[m.s ⁻¹]	[ft.s ⁻¹]	55.98 (183.6542)	56 (183.7245)
FW	[kg]	[lb]	156.91 (345.93)	156.96 (346.03)
FW_{added}	[kg]	[lb]	41.58 (91.67)	41.58 (91.57)
RNG_{max}	[nmi]		357.83	357.69
Endurance	[h]		3.75	3.75
HIGE	[m]	[ft]	5200.8 (17063.1)	4332.5 (14214.4)
HOG	[m]	[ft]	3687.6 (12098.6)	2719.5 (8922.1)
Service Ceiling	[m]	[ft]	6067.7 (19907.3)	5229.2 (17156.1)

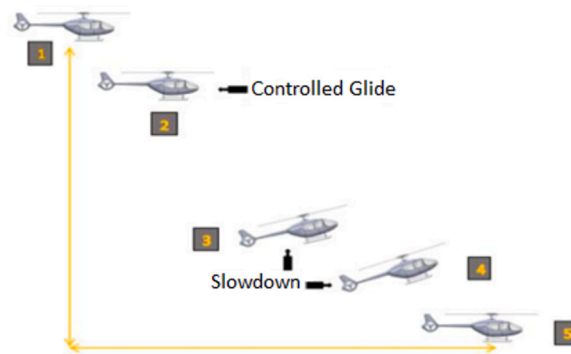


Fig. 21. Autorotation.

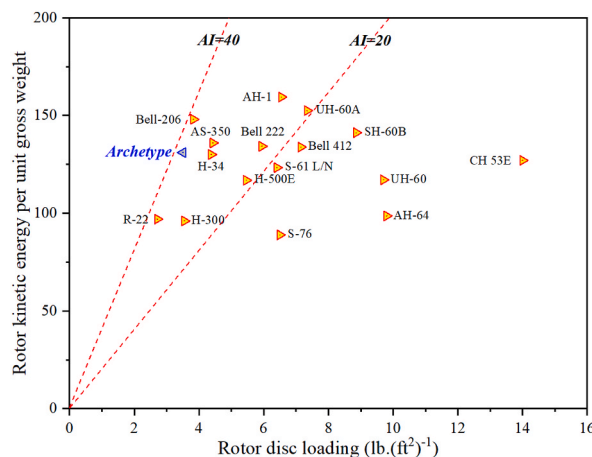


Fig. 22. An autorotation performance comparison chart.

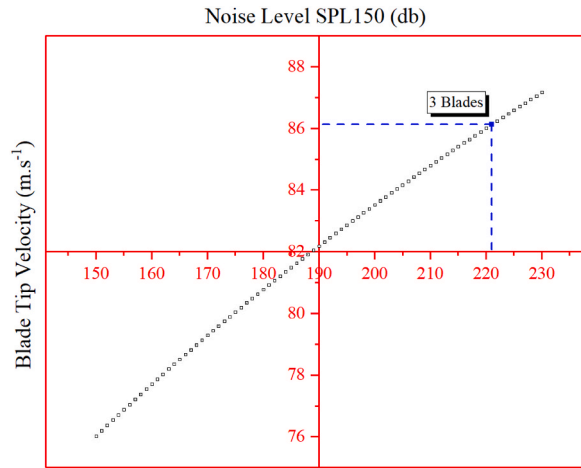


Fig. 23. Noise level based on the number of blades.

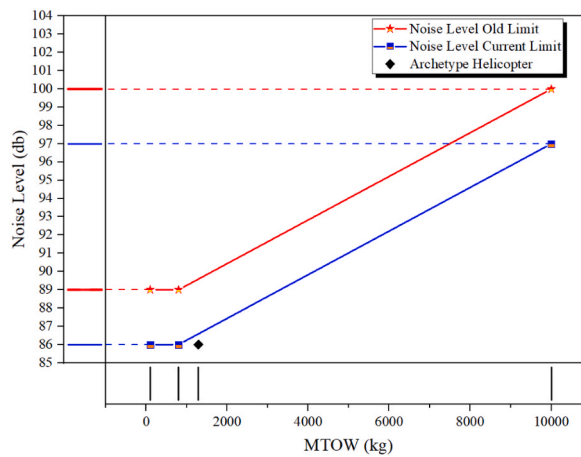


Fig. 24. CS-36 certification noise limit ranges.

the graph of the old and new noise limits depending on the CS-36 standards, and dependent on the maximum take-off weight. According to the figure, the archetypal helicopter, which has an environmentally friendly and sustainable design, meets the noise emissions level certification conditions. Additionally, innovative designs were followed in order to reduce noise in the designed helicopter. To reduce the noise level created by the tail rotor, a fan-type tail design was performed, with the aim being of reducing the noise level originating from the tail.

4.11. Stability calculations

A time-dependent examination of the helicopter’s response to impact determines the dynamic stability of the helicopter. Stability, maneuverability, and controllability result from the movement of the helicopter in three axes. Operations are performed by taking the center of gravity of the three axes as the reference point. Longitudinal stability involves the pitch motion of the helicopter moving on its horizontal axis. Lateral stability is expressed as the stability of the helicopter along its longitudinal axis. Stability on its vertical axis is called directional stability. To perform the stability and control analysis, the methods of Padfield [36] and Prouty [41] are acted upon.

Stability derivatives consist of force and moment derivatives concerning the vehicle’s translational velocities and angular velocities. For stability and control derivatives, the literature was searched and the values of the OH-6A model, which is a helicopter of a similar class and weight, were used [16]. The stability variants of the OH-6A helicopter for hover and forward flight at a speed of 130 knots are given in Table 11.

To solve the nonlinear equations of a helicopter with six degrees of freedom, linearization is first performed on a trim point. In this way, the behavior of the model is predicated. These equations are then expressed in state-space form. The general form of the state-space model of a system is in Eq. (3):

Table 11
Derivatives of stability.

Derivative	Hover	130 knot	Derivative	Hover	130 knot
X_u	-0.0257	-0.057	L'_u	0.001	0.0047
X_w	0.0113	0.0138	L'_w	-0.0064	-0.1655
X_q	0.3972	0.2905	L'_q	-1.136	-1.626
X_v	0.0004	0.0001	L'_v	-0.1516	-0.2542
X_p	-0.2494	-0.2578	L'_p	-4.9198	-4.8062
X_r	-0.0185	-0.024	L'_r	-0.2873	0.0213
Y_u	0.0158	0.0036	M'_u	0.0414	0.0498
Y_w	-0.0194	-0.048	M'_w	-0.0196	-0.0065
Y_q	-0.2573	-0.3196	M'_q	-1.7645	-2.9912
Y_v	-0.0435	-0.1438	M'_v	-0.0086	-0.1163
Y_p	-0.4104	-0.4203	M'_p	0.3763	0.1693
Y_r	0.1045	0.4176	M'_r	0.0719	0.6034
Z_u	-0.0422	0.0178	N'_u	-0.0861	-0.0301
Z_w	-0.3404	-0.8096	N'_w	0.1018	0.134
Z_q	0.005	-0.3092	N'_q	-0.1724	0.6085
Z_v	-0.044	-0.0485	N'_v	-0.0054	0.3405
Z_p	0.0177	-0.5825	N'_p	-1.0748	-0.8152
Z_r	0.4495	0.6244	N'_r	-0.8645	-2.643

$$\{\dot{x}\} = [A]\{x\} + [B]\{u\} \tag{3}$$

The matrices A and B contain the stability and control derivatives, respectively. Here, x is the state vector, u is the control input, A is the stability matrix, and B is the control matrix. The control vector u in this formulation includes the main rotor collective, the longitudinal and lateral loops, and the tail rotor collective.

Lateral and longitudinal stabilities are studied separately in Eq. (4):

$$A_{lat} = \begin{bmatrix} \frac{Y_v}{m} & \frac{Y_p}{m} & gc\varphi_0c\theta_0 & \frac{Y_r}{m} - u_0 \\ L'_v & L'_p & 0 & L'_r \\ 0 & 1 & 0 & c\varphi_0t\theta_0 \\ N'_v & N'_p & 0 & N'_r \end{bmatrix} \quad A_{long} = \begin{bmatrix} \frac{X_u}{m} & \frac{X_w}{m} & \frac{X_q}{m} - w_0 & -gc\theta_0 \\ \frac{Z_u}{m} & \frac{Z_w}{m} & \frac{Z_q}{m} - u_0 & -gc\varphi_0s\theta_0 \\ \frac{M_u}{I_{yy}} & \frac{M_w}{I_{yy}} & \frac{M_q}{I_{yy}} & 0 \\ 0 & 0 & c\varphi_0 & 0 \end{bmatrix} \tag{4}$$

The longitudinal and lateral motion equations were solved in a MATLAB code. The results of the code were the eigenvalues which give information about the helicopter modes. Fig. 25(a and b) and 26(a, b) show the estimated longitudinal and lateral poles for cruise flight at a speed of 130 knots. Fig. 25(a) presents the longitudinal as well as Fig. 25(b) shows the lateral of suspended flight stability

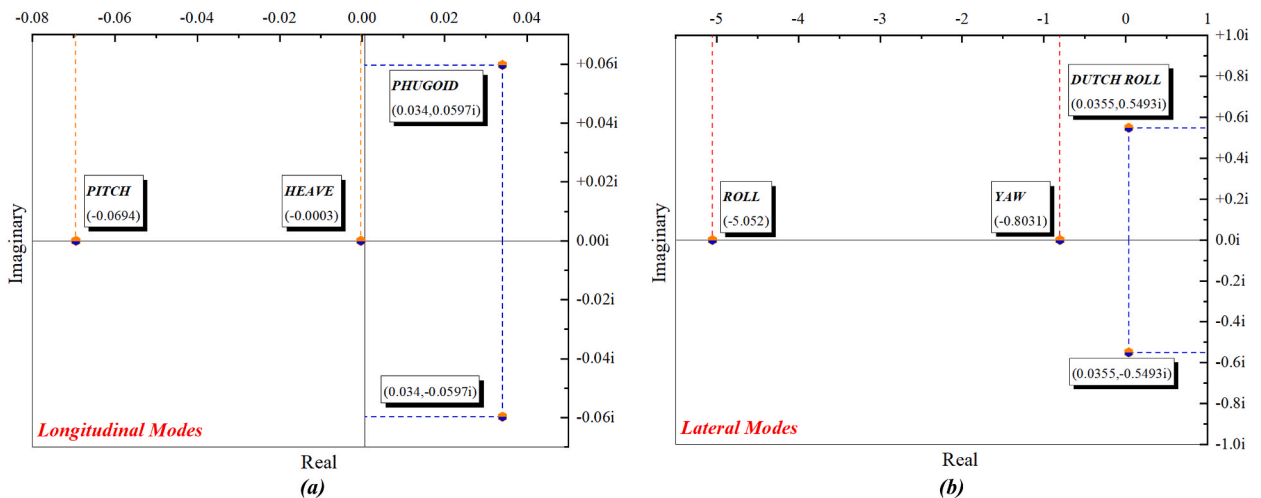


Fig. 25. Suspended flight stability modes; (a) longitudinal, (b) lateral.

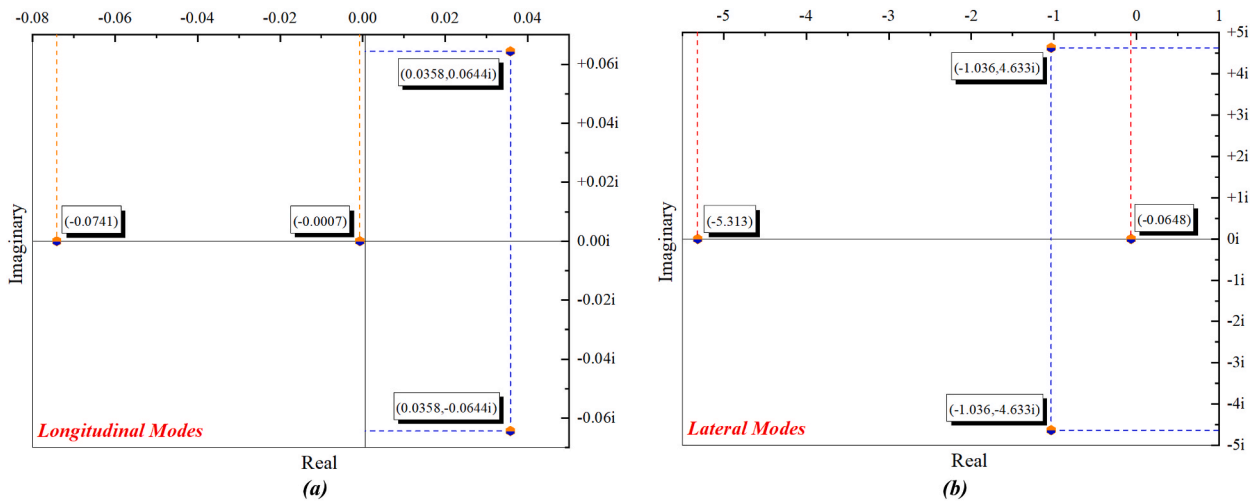


Fig. 26. Advanced flight modes at a speed of 130 knots; (a) longitudinal, (b) lateral.

modes. Moreover, Fig. 26(a) illustrates the longitudinal of advanced flight modes at a speed of 130 knots, on the other hand, Fig. 26(b) presents the lateral.

Phugoid and heave modes appear to be almost stable during hover and at 130 knots of level flight. Heave damping describes the vertical wind response and appears to become more stable as speed increases. The roll and pitch modes were stable in both flight conditions. This shows that the helicopter has good roll and pitch damping. The Dutch roll mode becomes more stable as speed increases. The roll mode was the most stable model. The size of the horizontal stabilizer affects stability. Increasing the planform area of the tail plane ensures speed stability and minimizes the nose-down position of the vehicle in forward flight. However, as the size of the horizontal stabilizer increases, the positive angle of attack tends to increase the archetypal helicopter’s flight control system, as seen in Fig. 27, which is a classic flight control system with collective, cyclical control, and pedal control. While collective control changes the amount of total carry over the rotor, cyclical control changes the direction of control using the gimbal. A gimbal is needed to transmit the controls given by the pilot to the main rotor.

There are two plates in this system. While the top plate can rotate, the bottom plate does not. Furthermore, the two can move upwards together. According to the ball joint in the middle, the main rotor can be angled towards the desired side with control coming from the pilot. When the collective lever is pulled up in the helicopter, the gimbal mechanism goes up, and the thrust increases. Changing the cyclical control changes the direction of the helicopter, depending on the angle in the gimbal mechanism. At the same time, thanks to the pedals, the nose of the helicopter can be pulled up or down. There is a scissor mechanism in the main rotor, which is connected to the rotor by a top plate. The reason for the existence of the scissors is to ensure that the top plate rotates with the rotor and that there is no obstruction. Therefore, the rotor can rotate in three directions according to the control of the pilot. Controls from the pilot rule to the hydraulic systems, and from the hydraulic systems to the gimbal. Because the pilot will have difficulty controlling using arm power, mixing mechanisms were used here.

4.12. Environmentally friendly and sustainable performance

In the light-class utility helicopter designed in this study, sustainability and environmental factors were largely taken into consideration to a great extent. In the table of determination of criteria for the whole design, the sustainability impact was determined at an extremely high level of 10%. Performance calculations, on the other hand, were made with considerable attention paid to sustainability and environmental impact, as well as consideration of numerous other parameters. Additionally, in terms of sustainability and environmentalism, helicopter scaling and structural design, including primary partition, beam, and support elements, were



Fig. 27. Flight control system.

designed as a system that transfers loads from the engine during flight operation and reaction forces from the ground during landing operations to the fuselage. In addition, when the general performance calculations, autorotation calculations, weight breakdown calculations, and noise emissions level calculations are examined, it can be seen that the system is designed to be environmentally friendly and sustainable.

As a result of calculations based on a number of parameters, it can be seen that the MTOW and empty weight values obtained as a result of this archetypal helicopter design are relatively low compared to equivalent helicopters. The low total and empty weight have led to a decrease in the fuel consumption of the helicopter design and made the system more environmentally friendly and sustainable. In addition, the archetypal helicopter has been designed with the aim of a minimum noise level during flight and operational steps for ecological purposes. As mentioned before, the objective of the research is to achieve a sustainable, ecologically friendly, and fuel-efficient design by reducing the number of accidents and damage.

5. Conclusion

Within the scope of this study, an environmentally friendly, economical, and ergonomic helicopter design is realized by considering numerous parameters. In addition to the determined mission profile and requirements, design requirements were established to obtain a sustainable, original, and high-performance helicopter design. Based on these requirements, a requirement matrix was created, and configurations were chosen by determining the impact ratios of the requirements. Within the scope of the methodology, weight and power calculations in the design study could be obtained within the scope of iterative processes. Authenticity was one of the most fundamental objectives in the design of the archetypal helicopter. A unique light-class helicopter design was obtained by comparing the performance parameters determined within the scope of the design study with competing products. Sub-systems were designed one by one as power transmission, control-avionics, rotor, propulsion, structural, and other sub-systems. CFD applications were used using the ANSYS program for blade profile selection and main rotor calculations, design, landing gear total deformation, and equivalent strain analysis and dimensioning calculations for the blade. In most of the general performance calculations, the MATLAB code was used over the formulas accepted in the literature. In summary, this study produced a completely unique, sustainable, and ergonomic light-class helicopter design by performing all performance calculations and considering numerous parameters. All the general features and dimensions selected for the design are shown in Table 12.

In summary, the design study, which was developed based on competitor product analyses and considering environmentalist features, revealed a helicopter design study with a similar passenger capacity, lower noise, lower emission level, high range, and innovative technologies. It is aimed at contributing to the literature by using innovative and environmentalist approaches within the scope of design. This contribution can be improved in many ways due to the wide range of design processes and helicopter design methodologies. Verification of the parameters determined in the helicopter design methodology with some flight and ground tests increases the convergence of the design methodology. The development of the design and the tests to be carried out in the future will make a significant contribution to the design literature.

In addition, it may be possible to further develop concepts such as control and stability as future plans within the scope of the

Table 12
General features of the design.

	General Specifications	Units	Values
Weight	MTOW	[kg]	1287.377
	Empty Weight	[kg]	588.89
	Fuel Capacity	[kg]	156.9
	Payload Capacity	[kg]	490
General Dimensions	Fuselage Length	[m]	9.33
	Fuselage Height	[m]	3.117
	Fuselage Width	[m]	1.6
	Landing Gear Width	[m]	2.124
	Horizontal Tail Surface Area	[m ²]	0.145
	Vertical Tail Arm	[m]	5.675
	Main Rotor Specifications	Disc Loading	[lb. (ft ²) ⁻¹]
	Blade Loading		0.067
	Blade Tip Velocity	[m.s ⁻¹]	221
	Blade Chord	[m]	0.243
	Blade Airfoil		SC-1095
	Blade Radius	[m]	4.852
	Blade Number		3
Tail Rotor Specifications	Blade Tip Velocity	[m.s ⁻¹]	136.91
	Blade Chord	[m]	0.103
	Blade Airfoil		NACA-0012
	Blade Radius	[m]	0.667
	Blade Number		6
Engine Specifications	Tail Configuration		Fenestron
	Power	[hp]	420
	Weight	[kg]	73.028
	Specific Fuel Consumption	[lbm.lbs.hr ⁻¹]	0.65

design. In addition, the design study has been developed with similar products in the literature, and the catalog of similar products can be further expanded and their performance characteristics improved. The authors of the study support all kinds of contributions to the literature and are open to all collaborations.

Author contribution statement

Enes Gunaltili: Conceived and designed the experiments; Analyzed and interpreted the data; Contributed reagents, materials, analysis tools or data; Wrote the paper.

Selcuk Ekici: Conceived and designed the experiments; Analyzed and interpreted the data; Contributed reagents, materials, analysis tools or data; Wrote the paper.

Abdullah Kalkan: Conceived and designed the experiments; Analyzed and interpreted the data; Contributed reagents, materials, analysis tools or data; Wrote the paper.

Faruk Esat Gocmen: Conceived and designed the experiments; Analyzed and interpreted the data; Contributed reagents, materials, analysis tools or data; Wrote the paper.

Utku Kale: Analyzed and interpreted the data; Wrote the paper.

Zeki Yilmazoglu: Analyzed and interpreted the data; Wrote the paper.

T. Hikmet Karakoc: Analyzed and interpreted the data; Wrote the paper.

Data availability statement

Data will be made available on request.

Declaration of competing interest

The authors declare that they have no known competing financial interests or personal relationships that could have appeared to influence the work reported in this paper

Appendix A. Supplementary data

Supplementary data to this article can be found online at <https://doi.org/10.1016/j.heliyon.2023.e17369>.

References

- [1] P.F. Pelz, P. Leise, M. Meck, Sustainable aircraft design — a review on optimization methods for electric propulsion with derived optimal number of propulsors, *Prog. Aero. Sci.* 123 (2021), 100714, <https://doi.org/10.1016/j.paerosci.2021.100714>.
- [2] F. Ekici, G. Orhan, Ö. Gümüş, A.B. Bahce, A policy on the externality problem and solution suggestions in air transportation: the environment and sustainability, *Energy* 258 (1) (2022), 124827, <https://doi.org/10.1016/j.energy.2022.124827>.
- [3] S. Ekici, Modeling joint parameters to make sense of helicopter induced emissions effects: greener rotorcraft, *AEAT* 93 (3) (2021) 366–383, <https://doi.org/10.1108/AEAT-08-2020-0164>.
- [4] F. Ali, I. Goulos, V. Pachidis, An integrated methodology to assess the operational and environmental performance of a conceptual regenerative helicopter, *Aeronaut. J.* 119 (1211) (2015) 67–90, <https://doi.org/10.1017/S0001924000010253>.
- [5] F. Sal, Simultaneous swept anhedral helicopter blade tip shape and control-system design, *AEAT* 62 (2) (2022), 022009, <https://doi.org/10.1108/AEAT-02-2022-0050>.
- [6] US Army Command, *Engineering Design Handbook Helicopter Engineering Part One Preliminary Design: (Helicopter Engineering AMCP 706-201, Preliminary Design)*, Eagle Eye Solutions, LLC; Part One edition, 1974.
- [7] U. Pietsch, G. Strapazzon, D. Ambühl, V. Lischke, S. Rauch, J. Knapp, Challenges of helicopter mountain rescue missions by human external cargo: need for physicians onsite and comprehensive training, *Scand. J. Trauma Resuscitation Emerg. Med.* 27 (1) (2019) 17, <https://doi.org/10.1186/s13049-019-0598-2>.
- [8] A.H. Rao, K. Marais, Comparing hazardous states and trigger events in fatal and non-fatal helicopter accidents, in: *16th AIAA Aviation Technology*, 2016, p. 67.
- [9] K. Sahu, A. Alzahrani F, K. Srivastava R, R. Kumar, Evaluating the impact of prediction techniques: software reliability perspective, *Comput. Mater. Continua (CMC)* 67 (2) (2021) 1471–1488, <https://doi.org/10.32604/cmc.2021.014868>.
- [10] K. Sahu, R.K. Srivastava, Predicting software bugs of newly and large datasets through a unified neuro-fuzzy approach: reliability perspective, *Adv. Math., Sci. J.* 10 (1) (2021) 543–555, <https://doi.org/10.37418/amsj.10.1.54>.
- [11] Defense Technical Information Center, *Engineering Design Handbook: Military Vehicle Electrical Systems*. Ft, Belvoir Defense Technical Information Center AMCP, 1974, pp. 360–706.
- [12] Baserga Claudio, Ingalls Charles, Henry Lee, Peyran Richard (Eds.), *Methodology for Estimating Helicopter Performance and Weights Using Limited Data*, ntrs. nasa.gov, 1990.
- [13] Q. Wang, Q. Zhao, Rotor aerodynamic shape design for improving performance of an unmanned helicopter, *Aero. Sci. Technol.* 87 (2019) 478–487, <https://doi.org/10.1016/j.ast.2019.03.006>.
- [14] R.G. Budynas, J.K. Nisbett, J.E. Shigley, *Shigley's Mechanical Engineering Design*, McGraw-Hill Education, New York NY, 2020.
- [15] M. Gagné, D. Theriault, Lightning strike protection of composites, *Prog. Aero. Sci.* 64 (2014) 1–16, <https://doi.org/10.1016/j.paerosci.2013.07.002>.
- [16] R.K. Heffley, W.F. Jewell, J.M. Lehman, R.A. Vanwinkle, *A Compilation and Analysis of Helicopter Handling Qualities Data*, vol. 1, 1979. Data compilation.
- [17] N. Zimmermann, P.H. Wang, A review of failure modes and fracture analysis of aircraft composite materials, *Eng. Fail. Anal.* 115 (2020), 104692, <https://doi.org/10.1016/j.engfailanal.2020.104692>.
- [18] Rolls Royce, M250 FIRST Network Directory, 2021. Indianapolis, Indiana 46206-0420.
- [19] Wayne Johnson, *Rotorcraft Aeromechanics*, Cambridge University Press, 2013.
- [20] S.G. Kee, *Guide for Conceptual Helicopter Design [Master's Thesis]*, Naval Postgraduation School, Canada, 1983.

- [21] M. Calvert, T-c Wong, Aerodynamic impacts of helicopter blade erosion coatings, in: 30th AIAA Applied Aerodynamics Conference, 2012.
- [22] Aadya Mishra, Sourav Pal, Prabhat Singh (Eds.), *Design & Vibration Analysis of Helicopter Main Rotor Blade*, tenth ed., 2020.
- [23] M.N. Tishchenko, V.T. Nagaraj, I. Chopra, Preliminary design of transport helicopters, *J. Am. Helicopter Soc.* 48 (2) (2003) 71, <https://doi.org/10.4050/JAHS.48.71>.
- [24] F. Savoye, P. Venet, M. Millet, J. Groot, Impact of periodic current pulses on Li-ion battery performance, *IEEE Trans. Ind. Electron.* 59 (9) (2012) 3481–3488, <https://doi.org/10.1109/tie.2011.2172172>.
- [25] F. Bazmi, A. Rahimi, Helicopter turboshaft engine database as a conceptual design tool, *SAE Int. J. Engines* 15 (1) (2022), <https://doi.org/10.4271/03-15-01-0003>.
- [26] L. Frizziero, L. Piancastelli, The installation of a common rail diesel engine on a light helicopter of the eurocopter EC120 class, *Ing. Inv.* 36 (1) (2016) 6–13, <https://doi.org/10.15446/ing.investig.v36n1.46221>.
- [27] Z. Dong, L. Liang, W. Zhang, L. Jiao, Di Peng, Y. Liu, Simultaneous pressure and deformation field measurement on helicopter rotor blades using a grid-pattern pressure-sensitive paint system, *Measurement* 152 (2020), 107359, <https://doi.org/10.1016/j.measurement.2019.107359>.
- [28] Y.-T. Choi, R. Robinson, W. Hu, N.M. Wereley, T.S. Birchette, A.O. Bolukbasi, et al., Analysis and control of a magnetorheological landing gear system for a helicopter, *J. Am. Helicopter Soc.* 61 (3) (2016) 1–8, <https://doi.org/10.4050/JAHS.61.032006>.
- [29] L.A. Powell, W. Hu, N.M. Wereley, Magnetorheological fluid composites synthesized for helicopter landing gear applications, *J. Intell. Mater. Syst. Struct.* 24 (9) (2013) 1043–1048, <https://doi.org/10.1177/1045389x13476153>.
- [30] Grigory Nesterenko, in: *Comparison of Damage Tolerance of Integrally Stiffened and Riveted Structures*, 2000.
- [31] J.M. Ernst, S. Schmerwitz, T. Lueken, L. Ebrecht, Designing a virtual cockpit for helicopter offshore operations, in: J.N. Sanders-Reed, J.J. Arthur (Eds.), *Degraded Environments: Sensing, Processing, and Display 2017*, SPIE, 2017, 101970Z.
- [32] Ananth Sridharan, Bharath Govindarajan, V.T. Nagaraj, Inderjit Chopra (Eds.), *Design Considerations of a Lift-Offset Single Main Rotor Compound Helicopter*, American Helicopter Society Aeromechanics Design for Vertical Lift, San Francisco, 2016.
- [33] Nik Mohd, Nik Ahmad, Ridhwan, Barakos George, *Comput. Aerod. Hovering Helicopter Rotors* 16–46 (2012).
- [34] J.G. Leishman, *Principles of Helicopter Aerodynamics*, second ed., Cambridge University Press, Cambridge, New York, 2006.
- [35] A. Charles, Jr. Yoerkie, Philip H. LeMasurier, Steven D. Weiner, *Helicopter Antitorque Device* 683 (1991), 904.
- [36] G.D. Padfield, *Helicopter Flight Dynamics: the Theory and Applications of Flying Qualities and Simulation Modelling*, American Institute of Aeronautics and Astronautics, Inc; repr., Washington DC, 1999, p. 1996.
- [37] R. Mouille, F. d'Ambra, *The 'fan-In-Fin': A Shrouded Tail Rotor Concept for Helicopters*, 1986, pp. 597–606.
- [38] Zlatko Petrović, Slobodan Strupar, Ivan Kostić, Aleksandar Simonović, Determination of a light helicopter flight performance at the preliminary design, *Stage* 51–60 (9) (2010) 535–543.
- [39] D.B. Schwinn, P. Weiland, M. Buchwald, Rotorcraft fuselage mass assessment in early design stages, *CEAS Aeronaut. J.* 12 (2) (2021) 307–329, <https://doi.org/10.1007/s13272-021-00492-z>.
- [40] P. Abbeel, A. Coates, T. Hunter, A.Y. Ng, Autonomous autorotation of an RC helicopter, in: B. Siciliano, O. Khatib, F. Groen, V. Kumar, G.J. Pappas (Eds.), *Experimental Robotics*, Springer Berlin Heidelberg, Berlin, Heidelberg, 2009, pp. 385–394.
- [41] R.W. Prouty, *Helicopter Performance, Stability, and Control*, Krieger Publishing Company, Malabar, Florida, 2005.